CHALMERS

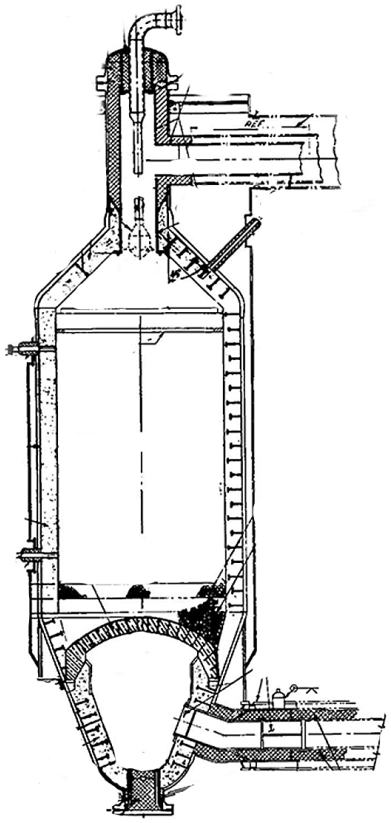

CFD Simulation of a Secondary Methane Reformer

Investigation of catalyst failure

Master of Science Thesis

JIMMY ANDERSSON
ISAAC NILSSON

Department of Chemical and Biological Engineering
Division of Chemical Engineering
CHALMERS UNIVERSITY OF TECHNOLOGY
Göteborg, Sweden, 2013

CFD Simulation of a Secondary Methane Reformer

Investigation of catalyst failure

JIMMY ANDERSSON
ISAAC NILSSON

Examiner:

Professor Bengt Andersson, Chemical Reaction Engineering, Chalmers University of Technology

Supervisor:

Ph.D. Muslikhin Hidayat, Gadjah Mada University

Ph.D. Rahman Sudiyo, Gadjah Mada University

Department of Chemical and biological engineering
Division of Chemical Reaction Engineering
CHALMERS UNIVERSITY OF TECHNOLOGY
Göteborg, Sweden 2013

CFD Simulation of a Secondary Methane Reformer

Investigation of catalyst failure

JIMMY ANDERSSON

ISAAC NILSSON

Department of Chemical and Biological Engineering
Division of Chemical Reaction Engineering
Chalmers University of Technology
412 96 Göteborg, Sweden
Phone + 46 (0)31-772 1000

Cover:
Modified drawings over the secondary reformer reactor

Göteborg, Sweden 2013

Preface

This thesis has been created through collaboration between Chalmers University of Technology (Gothenburg, Sweden), Gadjah Mada University (Yogyakarta, Indonesia), PT Pusri (Palembang, Indonesia) and with support of SIDA (Swedish International Development Cooperation Agency).

The scope of the project has been of technical, educational and social nature. The technical aspects relates to the investigation of an existing production unit, with help of the today best available methods and technologies. These methods and other skills have been transferred between the students, universities and corporations through the collaboration, where all has contributed to different parts. Finally an effort to understand each other's culture has been put in. This is important since multinational collaborations are crucial now days in many different areas, such as education, business and politics.

The thesis is a continuation of a previous work by M.Sc. Alfa Widyawan, an employee of PT Pusri. Throughout this project Mr. Alfa has contributed necessary information and data. The main part of the work has been carried out at Gadjah Mada University under supervision of Ph.D. Hidayat Muslikhin and Ph.D. Sudiyo Rahman. The project work has also been under supervision of Bengt Andersson, Chalmers University of Technology, who also is the examiner of the thesis.

The present report is divided into two parts. The first part focuses on the technical analysis of the studied process, while the second part discusses the cultural differences and our experiences of it.

Figure 1. This thesis has been created through collaboration between Chalmers University of Technology, Gadjah Mada University and PT Pusri.

CFD Simulations of a Secondary Methane Reformer
Investigation of catalyst failure
JIMMY ANDERSSON
ISAAC NILSSON
Department of Chemical and Biological Engineering
Chalmers University of Technology

Abstract

Fertilizer products are important supplements in modern agriculture. An increased demand for fertilizers is expected in developing countries due to increased population, higher living standards and urbanization. Such trends would increase the significance of efficient, local large scale production facilities. This master thesis investigates an actual reactor problem occurring in an auto thermal methane reformer operating in a urea production plant ran by the Indonesian corporation PT Pusri. The main issues involve catalyst damages and refractory bricks breakage in the middle top region of the catalyst bed, as well as elevated concentrations of unreacted methane exiting the reactor.

2D and 3D CFD simulations of the reactor geometry were carried out in order to study possible underlying factors. Numerical analysis were supported or extended by theoretical literature studies.

Obtained results indicate a mixing problem with substantial radial variations of temperature and methane concentration across the catalyst bed surface. Additionally a strongly impinging flow situation could be observed in the combustion zone. The burner design was shown to significantly influence flow pattern and distribution while turbulent inlet properties were insignificant.

It is believed that inadequate burner design is the source to the reactor problems observed. Impinging flow may exert large strain rates on the refractory bricks and once they are damaged the catalyst is exposed to the high temperature flame. Outdated burner design is also a major factor causing the insufficient mixing which may result in lowered methane conversion. However, without investigating the possibility of bad quality material no definite conclusion can be drawn.

An additional learning objective was the cultural exchange from a 4 month stay in Yogyakarta, Indonesia.

Keywords: secondary methane reformer, CFD, catalyst failure

Acknowledgement

We would like to mention a number of people who have been involved in the realization and working process of this project and thank them for their support and help.

- Bengt Andersson Supervisor and examiner
- Ronnie Andersson Supervision
- Dedi Eko Practical details and accompanied us at Gadjah Mada University
- Björn Lundberg Support and company
- Claes Niclasson Arranged contact with Gadjah Mada University
- Alfa Widyawan Company contact
- Hidayat Muslikhin Supervision in Indonesia
- Sudiyo Rahman Supervision in Indonesia

Moreover we are very grateful of Gadjah Madah University and PT Pusri for giving us the opportunity to come to Indonesia and do this thesis. We also want to thank SIDA for providing us financial aid.

Contents

1 Introduction

Production and use of various fertilizers is important in the modern society all around the world. It is often based on old and well-known processes and techniques that has been developed and tested through centuries.

PT Pusri is an Indonesian company located on the Sumatra and a major producer of fertilizers for the local market. The main product is urea which is one of the most used in the world today.

1.1 Agriculture and fertilizers

Production of food and other agricultural products around the world is expected to increase during the coming centuries. An increased demand can mainly be connected to increased population, growing middle class, increased use of bio-products etc. This, together with the fast urbanization around the world, creates a pressure on remaining farmers to produce more and more. The problem is not new and for years countries around the world have been trying to resolve this issue by boosting the efficiency in its agriculture in various ways such as: introduce machines instead of horses, breeding of better crops, introduce fertilizers etc. All this together is the foundation for the modern agricultural system.

Usage of fertilizers has been criticized of many environmental groups around the world for being harmful to the environment. Fertilizers create eutrophication, soil depletions and contribute to the greenhouse effect. The criticism is important, but can to some extent be met by more responsible use of it. But the production of fertilizers is often connected to high energy consumption and it is estimated that about 1.2% of the world's energy consumption (Swaminathan & Sukalac, 2004) is used in this production; mainly with natural gas as stock feed. Therefore is it of uttermost importance to run the factories as efficient as possible.

A ban on fertilizers is not realistic with the agricultural methods known and used today. Topsoe (constructor of fertilizer plants) says on its website that "only 2/5 of the current global population could be nourished" without industrial ammonia (Topsoe, 2013). The issues mentioned are already today addressed by regulations and a high price on fertilizers; a price that most likely will increase due to an increase in price for production of natural gas.

The process that was investigated in this project is located in Indonesia, where needs for fertilizers are steadily increasing with the modernization of the agriculture. Today Indonesia is the 4^{th} most populous country in the world and the 10^{th} largest agricultural producer. The farmers consist of in total 42 million people and covers 38% of the population. Development in the country proceeds fast, which also includes the agriculture. But in a country where half of the population lives under 2 USD PPP a day fertilizers is not available for everyone. To address this, the government subsidizes fertilizers for small farmer.

1.2 PT Pusri

In a city called Palembang on the island of Sumatra, Indonesia, the company PT Pusri (Pupuk Sriwijaya) is located. The corporation is state owned and was established in 1959 to produce fertilizers for the domestic market. Over the years several new production lines have been built to produce fertilizers in form of urea.

Today the corporation has about 2 700 employees and a capacity of producing 2.3 million tons urea per year. The plant is planning further expansion by building one additional production unit that will start to operate in 2015.

1.3 Urea

There are today many different fertilizers on the market. Some of these are organic ones and can use e.g. animal manure while others are inorganic. Urea is of the latter type and is one of the dominating products on the market today. The favors of urea compared to its competitors are connected to its high content of nitrogen, 46%, which is highest of all granular fertilizers. Compared to others it is usually less corrosive, but can be more expensive to use. (Lee., 2006) The use of urea in agriculture is currently increasing around the world.

1.4 Problem formulation

In 2011 PT Pusri encountered problems in the secondary methane steam reformer reactor operating in their ammonia production line Pusri-II.

The primary issue is related to concentration levels of unreacted methane exiting the reactor being significantly higher than expected. Underlying factors to this problem is believed to be insufficient mixing of the ingoing process gas and air resulting in an uneven methane concentration distribution into the catalyst bed.

An observed secondary issue is that the protective refractory brick layer located before the catalyst bed breaks and result in severe catalyst damages in the center part of the catalyst bed surface. The problem is believed to originate from a highly uneven temperature profile across the catalyst surface.

PT Pusri has attempted to resolve the problems by some means. One of them was to decrease the catalyst load so that the distance between the burner and the catalyst bed was increased, giving the reagents more time to mix. The water content in the air stream was also increased in an attempt to favor the consumption of methane in the steam reforming reactions. Apparently none of them gave any significant improvement and the problem remains unresolved.

1.5 Preceding master thesis

A preliminary CFD study of the reactor problem was carried out by Alfa Widyawan. His work was limited to 2D simulations of the combustion zone, disregarding the catalyst bed. Presented results in this study indicated an uneven temperature profile on the catalyst surface with higher temperature regions located in the center of the reactor. The maximum temperature of the flame reached 1600 °C which is still below the maximum allowed operation temperature (1800°C) of the refractory bricks that are arranged in a layer before the catalyst bed. The reactor behavior was further studied through sensitivity analysis by varying; gas inlet mass flow, air inlet temperature, distance between burner and catalyst bed and finally manipulating the burner air inlet angle. It was concluded that most cases deviating from the standard case would give inferior methane conversion and or more uneven distribution. Only displacing the catalyst bed, increasing the time for reagents to mix would result in a more even distribution across the inlet to the catalyst surface.

However, objections on the validity of obtained results can be raised. Several errors were found in mass flow inlet conditions and minor deviations in geometry measurement from the actual burner drawings.

In the final part of the report Alfa states a number of suggestions for continued work on the problem:

- Investigate material quality of refractory layer of bricks
- Install a thermocouple at the end of the combustion zone to validate simulation results
- Extend study with 3D simulations
- Evaluate alternative burner designs to reach optimal concentration and temperature distribution into the catalyst
- Simulate the whole secondary reformer, including the catalyst zone and the catalytic reaction
- Include radiation effects in the heat transfer model

1.6 Present master thesis

The present master thesis evolved through the above conclusions made by Alfa. Focus was laid upon correcting geometry and inlet conditions as well as validating a reactor model in 2D for subsequent application in 3D simulations. Additionally the catalytic bed, including the steam reforming reactions, was modeled and simulated in an attempt to recreate the complete reactor. The technical goal of the project is to gain a better, and more realistic, understanding of the reactor behavior and possible underlying causes of the actual problems.

2 Theory

2.1 Production of Urea

The dominating process for producing urea in the world is also the process that can be found at PT Pusri. Natural gas is used as feed stock and in the other end of the process urea in the form of white solid granulates (which is not true since PT Pusri colors theirs pink) is the final product.

Before entering the process natural gas is purified, where impurities such as sulfur are removed. Clean natural gas is passed into a two steps steam reformer where synthesis gas is produced. Through the Haber-Bosch process the hydrogen produced in the reformer section further reacts with nitrogen to form ammonia through the reaction:

$$3H_2 + N_2 \rightarrow 2NH_3 \qquad 2\text{-}1$$

The ammonia is then converted with carbon dioxide to form urea through the Bosch-Meier process:

$$2NH_3 + CO_2 \rightarrow (NH_2)_2CO + H_2O \qquad 2\text{-}2$$

Finally granulates are formed by removal of water. The real process consists of many sub steps, but the process is well-known and used all around the world today.

2.2 Reforming techniques

The process of reforming natural gas into synthesis gas has been extensively studied for more than 60 years and a number of different technologies are applied in today's industry (Dybkjaer, 1995). Even though the methods have been present for a long time the technologies are still evolving within areas of equipment design and catalysts. The following subchapter briefly summarizes the state-of-the-art of these reforming technologies.

The main reforming reactions are highly endothermic, which leads to that additional heat needs to be added in order to attain a high conversion. How this heat is added to the process is one of the key aspects that differentiate the different technologies used in industry today.

i. Tubular, fired reforming: catalyst filled tube bundles are placed inside a furnace with burners located on the top, bottom or sides on the inner walls of the furnace. This way the required heat is supplied by external combustion through the tube walls.
ii. Heat exchange reforming: the process stream is led through a heat exchanger unit to provide the heat required in the reforming process.
iii. Adiabatic pre-reforming: an adiabatic fixed bed reactor is located upstream of an ordinary tubular reformer.
iv. Auto thermal reforming and secondary reforming: an auto thermal reactor is divided into two parts consisting of a combustion chamber followed by a catalyst bed. In the combustion chamber methane reacts with oxygen and releases the heat that is required for the catalytic reactions in the following bed.

Normally tube reactors are used in primary reformers while auto thermal reactors are commonly used in secondary reformers. The pre-reformer is used to reduce higher hydrocarbons into carbon oxides, hydrogen and methane by using a highly active reforming

catalyst. Another advantage is that the low operation temperature favors chemisorption of sulfur on the catalyst resulting in a sulfur-free feed gas into the tubular reformer. With no risk of sulfur poisoning, the tubular reformer catalyst will have an increased life time and reduced risk of hot spots in the bed.

2.3 Auto thermal secondary reformer

This thesis focuses on the secondary reformer which follows the primary reformer and is used to increase the conversion of methane. PT Pusri operates an auto thermal steam reformer in which the gas is partially burned in a primary combustion zone and heat is released. Thereafter the gas flows into a catalytic bed where the endothermic steam reforming reactions occur.

In the burner section several combustion reactions take place. There are mainly two species in the inlet that will contribute to this reaction, namely hydrogen and methane. The overall reactions can be summarized into (Yu, 2002):

$$H_2 + \frac{1}{2}O_2 \rightarrow H_2O \qquad 2\text{-}3$$

$$CH_4 + O_2 \rightarrow CO + H_2O + H_2 \qquad 2\text{-}4$$

$$CH_4 + 2O_2 \rightarrow CO_2 + 2H_2O \qquad 2\text{-}5$$

As for the steam reforming reactions occurring in the catalytic section there are various different proposed reaction mechanisms. Three global reactions are however to be considered to be dominant for steam reforming (Xu & Froment, 1989):

$$CH_4 + H_2O \leftrightarrow CO + 3H_2 \qquad 2\text{-}6$$

$$CO + H_2O \leftrightarrow CO_2 + H_2 \qquad 2\text{-}7$$

$$CH_4 + 2\,H_2O \leftrightarrow CO_2 + 4\,H_2 \qquad 2\text{-}8$$

2.4 Catalytic bed

The second part of the reactor consists of catalyst particles in the shape of perforated cylinders that are placed in random order as a packed bed. The cylinders are all equal and are illustrated in Figure 2.

Figure 2. The catalyst consists of cylinders with the dimensions 16.5 x 18.0 mm which are perforated with holes of 7 x 3.4 mm

A catalyst bed is used to increase the conversion speed of certain reactions. The particles are fabricated from porous gamma-alumina covered with an active layer consisting of nickel (for product specification see Appendix: Catalysis specification).

The reactor pressure drop through this catalytic bed can be estimated from Erguns law:

$$\frac{|\Delta p|}{L} = \frac{150\mu}{D_p^2}\frac{(1-\epsilon)^2}{\epsilon^3}v_\infty + \frac{1.75\rho}{D_p}\frac{1-\epsilon}{\epsilon^3}v_\infty^2 \quad 2\text{-}9$$

Estimations of the pressure drop will be important to include in the CFD simulations. One way is to divide the components in Erguns law into two: one that treats the inertial resistance and one that consider the viscous resistance. These two can be seen in (2-10) and (2-11) respectively:

$$C_1 = \frac{150}{D_p^2}\frac{(1-\epsilon)^3}{\epsilon^3} \quad 2\text{-}10$$

$$C_2 = \frac{3.5}{D_p}\frac{1-\epsilon}{\epsilon^3} \quad 2\text{-}11$$

Another important catalytic bed parameter is the bed porosity which is defined in (2-12).

$$\gamma = \frac{V_{cat}}{V_{tot}} \quad 2\text{-}12$$

Flow behavior through a catalytic bed will be heavily influenced of the physical space that the material occupies. This is most significant in radial coordinates and should thus be included. One common way of modeling this feature is by considering the movements as a (mechanical) radial dispersion. Many researchers have looked into this issue and in general propose that a radial Péclet number of 11 (Schnitzlein, 2001) for packed bed flows. This gives an expression for radial dispersion according to:

$$D_{radial} = \frac{LU}{Pe_L} \quad 2\text{-}13$$

To verify if the radial dispersion is of importance in the present case the relevant time scales for the radial dispersion and axial transport is compared. According to (Rasmusson A, 2010) the relevant time constants can be defined as:

$$\tau_{axial} = \frac{L}{v_z} \quad 2\text{-}14$$

$$\tau_{radial} = \frac{R^2}{D} \quad 2\text{-}15$$

2.5 Deactivation of catalyst

All catalysts will be deactivated over time. Some catalysts deactivates in seconds, while other last for years. In this case will sintering, coking and poisoning be the three most important aspects to consider regarding deactivation. Poisoning will be left out since the plant removes the sulfur before the gas reaches the reformer and therefore not be problem under regular process conditions.

2.5.1 Sintering

One of the major mechanisms for deactivation of the catalyst is sintering. Sintering is a process where the active surface area will decrease due to the formation of larger particles through the merge of smaller ones. Due to (Sehested, Gelten, Remediakis, Bengaard, & Nørskov, 2004) there are mainly three mechanisms behind sintering:

i) Particle migration – Hole crystallites migrates over the support and follows of coalescence

ii) Ostwald ripening – metal atoms are migrating over the surface and captured by crystallites
iii) Vapor transportation

The report suggest that the particle migration is the dominating one at low temperatures and that at temperatures above 600°C (40 bars) or 700°C (1 bar) Oswald ripening will become of importance. This is because the Oswald ripening has a higher activation barrier.

Sintering is dependent on the particle size (smaller tends to increase the rate) and to the composition of the gas. It is proposed that the rate is proportional to $P_{h2}/P_{h2o}^{0.5}$, where the rate increases with respect to the water content is related to the –OH bounding's on the surface of the catalyst.

2.5.2 Coking

As mentioned in the kinetics chapter (see below), the occurrence of char forming reactions was discussed by Xu and Froment in terms of thermodynamical analysis and it was concluded that they can be rejected from the kinetics model. In reality however, coking is a widespread problem in industrial methane reforming.

Nickel catalysts are known to catalyze the formation of coke and may lead to catalyst deactivation by coverage of nickel surface sites or blockage of pore entrances (Rostrup-Nielsen, 1975) (Trimm, 1997). As mentioned previously the steam reforming process comprise mainly endothermic reactions. This means that a local cooling effect can be expected as a result of these reactions. A deactivation of the catalyst could therefore lead to an increase in surface temperature at the catalyst and therefore damages.

The process of coke deposition is believed to originate through thermal cracking or catalytic reactions involving the same intermediates as are involved in the main reforming reactions (Trimm, 1997). The overall coking reactions can be described according to (2-16) to (2-18).

$$CH_4 \rightleftarrows C + 2H_2 \qquad 2\text{-}16$$

$$2CO \rightleftarrows C + CO_2 \qquad 2\text{-}17$$

$$CO + H_2 \rightleftarrows C + H_2O \qquad 2\text{-}18$$

The formation of coke through the last two reactions will be less favored in high temperature ranges. However, the forward step of the first reaction is favored by increased temperature. Thus methane dissociation on the metal surface will be the most prevalent source to carbon deposition in steam reforming.

The occurrence of coke formation would be indicated by an increase in reactor pressure drop due to accumulated char blocking the catalyst bed. In case of severe coking the problem can be minimized by addition of sulfur or other metals (Trimm, 1997).

2.6 Kinetics

As previously stated the methane reforming process is well established and has been extensively studied. One of the main areas subject to research has been the reaction kinetics. It is of central importance not only for understanding fundamental mechanisms but also due to the fact that reactor and equipment must be designed with respect to the nature of reaction kinetics. Proposed mathematical kinetic models in literature may be further implemented in

reactor simulations in order to study a wide range of reaction phenomena such as heat transfer and mixing of reactants.

Methane steam reforming is a catalytic reaction and nickel catalysts supported on alumina is commonly used in industry. However studies carried out on new catalysts has revealed that catalysts with small quantities of noble metals (Pt, Pd, Ir) can increase the methane conversion in experimental ATR systems by increasing the metal surface area available for reaction (Dias & Assaf, 2008).

In the remaining part of this chapter a literature review on the fundamental reaction kinetics for methane steam reforming will be carried out and discussed.

One of the most commonly implemented kinetic models in scientific reactor simulations was proposed by Xu and Froment (Xu & Froment, 1989) (Chan, Hoang, & Ding, 2005) (Fazeli & Behnamy, 2007) (De Wilde & Froment, 2012). Three sets of rate equations were derived through thermodynamical analysis in combination with laboratory experimental findings. The experiments were carried out in a plug flow reactor in temperature ranges of 773-823 K and pressure ranging from 3 to 15 bars. Initially 11 possible global reactions for methane steam reforming were suggested, among them coking reactions, but thermodynamic analysis reduced them to 3 main reactions presented in Table 1 below.

Table 1. Overall reactions occuring in methane steam reforming with corresponding reaction enthalpy

Number	Reaction	ΔH_{298}, kJ/mol
1	$CH_4 + H_2O \rightleftarrows CO + 3H_2$	+ 206.1
2	$CO + H_2O \rightleftarrows CO_2 + H_2$	- 41.15
3	$CH_4 + 2H_2O \rightleftarrows CO_2 + 4H_2$	+ 165.0

Some other researchers have preferred to exclude the water-gas shift reaction (number 2) from their models (Avetisov et al., 2010) (De Deken J, Devos E, & Froment G, 1982) with the motivation of it not having much effect on the final outcome. Note the highly endothermic nature of reaction 1 and 3 and the slightly exothermic water-gas shift.

Xu and Froment further elaborated their model by developing a steam methane reforming reaction mechanism consistent with literature and experimental observations. The reaction mechanism describes the overall reactions by elementary steps on a molecular level. In order to discriminate the model and develop a final reaction scheme a number of qualified assumptions were made.

1. H_2O reacts with surface nickel atoms producing adsorbed oxygen atoms and gaseous hydrogen
2. CH_4 is adsorbed on surface nickel atoms and reacts either with adsorbed oxygen or through dissociation into chemisorbed radicals (CH_3-$*$, CH_2-$*$, CH-$*$, C-$*$) where $*$ is an active surface site on the catalyst
3. The surface concentrations of carbon-containing radicals are lower than the total concentration of the active sites
4. Chemisorbed oxygen and carbon-containing radicals reacts to form $*$-CH_2O, $*$-CHO, $*$-CO_2 or $*$-CO.

5. Formed hydrogen is desorbed into the gas phase and/or is in equilibrium with adsorbed hydrogen (H-∗, H_2-∗)
6. The reaction mechanism has a step for reactions 1, 2 and 3 which is significantly slower than the other steps so that it may be regarded as rate controlling step for the corresponding overall reaction.

With these assumptions as a base the elementary steps presented in Table 2 were established along with a single selected rate determining step (rds) for each of the global reactions 1-3.

*Table 2. Elementary steps of the developed reaction mechanism where * is a free active site on the nickel catalyst surface.*

Elementary step					
H_2O	$+ *$	$\rightleftarrows$	O-∗	$+ H_2$	
CH_4	$+ *$	$\rightleftarrows$	CH_4-∗		
CH_4-∗	$+ *$	$\rightleftarrows$	CH_3-∗	$+ H$-∗	
CH_3-∗	$+ *$	$\rightleftarrows$	CH_2-∗	$+ H$-∗	
CH_2-∗	$+ O$-∗	$\rightleftarrows$	CH_2O-∗	$+ *$	
CH_2O-∗	$+ *$	$\rightleftarrows$	CHO-∗	$+ H$-∗	
CHO-∗	$+ *$	$\rightleftarrows$	CO-∗	$+ H$-∗	rds reaction 1
CO-∗	$+ O$-∗	$\rightleftarrows$	CO_2-∗	$+ *$	rds reaction 2
CHO-∗	$+ O$-∗	$\rightleftarrows$	CO_2-∗	$+ H$-∗	rds reaction 3
CO-∗		$\rightleftarrows$	CO	$+ *$	
CO_2-∗		$\rightleftarrows$	CO_2	$+ *$	
$2H$-∗		$\rightleftarrows$	H_2-∗	$+ *$	
H_2-∗		$\rightleftarrows$	H_2	$+ *$	

Rate equations were subsequently derived for the global reaction 1-3 in terms of each corresponding rate determining step. The rate equations were further manipulated with the Langmuir equilibrium relations to eliminate the concentrations of the adsorbed species so that the reaction rate could be expressed in gas bulk concentrations. Below are the final derived rate equations for reactions 1-3.

$$r_1 = \frac{k_1}{p_{H_2}^{2.5}}\left(p_{CH_4}p_{H_2O} - \frac{p_{H_2}^3 p_{CO}}{K_1}\right)/(DEN)^2 \qquad 2\text{-}19$$

$$r_2 = \frac{k_2}{p_{H_2}}\left(p_{CO}p_{H_2O} - \frac{p_{H_2}p_{CO_2}}{K_2}\right)/(DEN)^2 \qquad 2\text{-}20$$

$$r_3 = \frac{k_3}{p_{H_2}^{3.5}}\left(p_{CH_4}p_{H_2O}^2 - \frac{p_{H_2}^4 p_{CO_2}}{K_3}\right)/(DEN)^2 \qquad 2\text{-}21$$

Where K_i is the equilibrium constant of reaction i and the numerator

$$DEN = 1 + K_{CO}p_{CO} + K_{H_2}p_{H_2} + K_{CH_4}p_{CH_4} + K_{H_2O}p_{H_2O}/p_{H_2} \qquad 2\text{-}22$$

Where K_j is the adsorption equilibrium constant of component j.

The rate constants and adsorption equilibrium constants were fit to experimental data and were found to satisfy the Arrhenius equation and van't Hoff equation respectively. From these

equations pre-exponential coefficients could be determined. Relevant kinetic data such as pre-exponential coefficients and activation energies can be found in the referred article.

The reaction rate of formation or consumption for each component can be described in terms of the main reaction rate equations (2-19) to (2-21) according to the following expressions

$$-r_{CH_4} = r_1 + r_3 \quad 2\text{-}23$$

$$-r_{H_2O} = r_1 + r_2 + 2r_3 \quad 2\text{-}24$$

$$r_{CO} = r_1 - r_2 \quad 2\text{-}25$$

$$r_{CO_2} = r_2 + r_3 \quad 2\text{-}26$$

$$r_{H_2} = 3r_1 + r_2 + 4r_3 \quad 2\text{-}27$$

A.K. Avetisov et al published an article in 2010 (Avetisov et al., 2010) where steady-state kinetics of steam methane reforming over nickel catalysts was studied. The approach of their work was to critically review known kinetic models and propose a new, improved microkinetic model based on new and old experimental data. Their discussion on the kinetic model by Xu and Froment reveals some model inadequacies. First of all the formation of carbon monoxide model do not agree with experimental results due to faults in the procedure of rate constant fitting. This issue was corrected in the model proposed by A.K. Avetisov et al in the paper. However, the authors also criticized the suggested mechanism arguing that methane adsorption to the catalyst (CH_4-*) is unlikely without dissociating into CH_3-* and H-*, which was shown to be an accurate statement by Aparicio (Aparicio, 1997). From the review of previously presented models along with new experimental data a modified highly complex model was formulated by the authors.

Despite of the exposed shortcomings of the kinetic model suggested by Xu and Froment it was selected as reaction model in the performed CFD simulations with the motivation of being well cited and implemented in numerous previous methane reforming simulations and also due to the article completeness of ingoing parameters such as pre-exponential coefficients and activation energies.

2.7 Diffusional reaction limitations

Xu and Froment used a crushed catalyst with particle sizes ranging from 0.18 to 0.25 mm in size in their laboratory experiments. For industrial application the catalyst particle are significantly larger and consequently it is advised that diffusive mass transport limitations is accounted for. Another fact that supports mass transport limitations is that the industry process is carried out at high temperature ranges around 1000-1500K while the implemented kinetics model is fitted for experiments carried out in maximum temperatures of 823K. Thus direct application of the reaction expressions and rate constant would result in highly overestimated reaction rates. Two different kinds of mass transport phenomena should be considered. First there is the external film diffusion transport from the gas bulk to the catalyst surface and secondly the intraparticle pore diffusion inside the catalyst. According to Dybjaer the reforming reactions are mainly controlled by the external mass transport from bulk to the catalyst surface, which is the reason why high space velocities can be used in the process (Dybkjaer, 1995). This was considered valid for our simulations and intraparticle mass transport resistance was neglected.

Most scientific works however, include both the external and internal mass transport limitations (Chan et al., 2005). Such micro-scale accuracy is regarded as unnecessary for the scope of the present project and our approximations are considered valid.

The mass transfer resistance can be estimated by a number of different correlations. A simplification is to set a constant global efficiency factor for the whole system (which can be corrected to real process data). Such a factor will ignore effects from temperature, pressure and individual species characteristics. However, when these factors are stable through the catalyst, a global efficiency factor can be considered a valid assumption.

2.8 Heat transfer

Large temperature differences between the solid catalyst and the fluid gas may be present in the catalytic bed. In this case where the reactions are endothermic it is expected that the catalyst will have a slightly lower temperature than the surrounding gas. Therefore it is of importance to estimate the heat transfer between the catalyst and the fluid gas.

The heat transfer coefficient can be estimated by the Nusselt number according to (2-28). The Nusselt number itself can easiest be found by correlations (2-29) specifically developed for these kind of flows.

$$Nu = \frac{h * d_p}{k_f} \qquad 2\text{-}28$$

$$Nu = \frac{1.09}{\varepsilon} * Re^{\frac{1}{3}} * Sc^{\frac{1}{3}} \qquad 2\text{-}29$$

2.9 Mixing

To get two species to react with each other, it is required that they meet each other. This means that a good mixing is important to achieve an efficient conversion of reagents. Mixing can be characterized by the Dahmköhlers number, Da (Andersson et al., 2012).

$$Da = \frac{Typical\ time\ required\ for\ mixing}{Typcial\ time\ required\ for\ chemical\ reactions} \qquad 2\text{-}30$$

There are three general mixing situations: for low value Da the relative mixing rate will be fast and the kinetics will limit the reactions. For mediate and high Da on the other hand mixing will influence the outcome heavily and classic reactor models will be inadequate. For very high Da values, kinetics may be neglected and the reactions can be considered as a pure mixing problem.

To understand mixing phenomena, knowledge about both macro and micro level is crucial. On a macro level it is easy to see that parts of a reactor can have more or less of a certain species. E.g. in a tubular reactor concentration of a reactive species will be high in the inlet and low near the outlet, which means that the species on a macro level will have a bad mixing. But for example in a tank reactor where the mixing on a macro level is good (hopefully), there might be issues on a micro level. By the use of advanced measurements techniques it is possible to study mixing on a micro level; there might be lamellas that separate the species from each other. This has to be modeled in order to understand how fast the reactions will proceed.

In this project mixing is expected to be important, since the burning section consists of non-premixed inlets and fast reactions. Therefore it is probable that the geometry and setup of the burner will influence mixing and therefore the outcome.

2.10 CFD

Systems containing fluids be hard to predict regarding dynamics and structures. One method is to divide the system into small cells and resolve the flow for each cell individually in an iterative manner. This is usually referred to as CFD – Computational Fluid Dynamics.

During the last decade CFD has increased in importance since new models has been developed combined with more powerful computers for each year. The use of CFD tends to become very computationally expensive and force the engineer to choose between computational cost and accuracy. This means that while the cost for computers decreasing, the interest for these kinds of investigations will increase. The potential is however large and CFD is widely applied in different areas as nuclear power plants, aviation industry and process industry.

Accuracy of simulations is dependent on the grid size, the methods used, numerical schemes etc. Research in this area is progressing fast and leads to new and better models each year. But the reality is often very complicated and even for common engineering problems only crude estimations are possible to perform with CFD. There is a still large room for development of better models, combined with more powerful computers. But even if the validity can be questioned the results may predict many important aspects and phenomena.

2.10.1 Mesh

The concept of CFD is based on that the physical space is divided into smaller subspaces. The net that forms these subspaces is referred to as the mesh and consists of a large amount of computational cells. Since the equations are solved in each of these cells, the creation of the mesh is a key component in CFD. A mesh of low quality can introduce unnecessary large errors in the estimations, or even lead to inability to converge the solution.

A mesh can consists of cells in 2D or 3D and be of various geometric layout such as triangles and hexahedrons. The quality of the mesh depends on what shape the cells have, how they are arranged related to the flow and the size of them. The smaller the computation cells are, the more details can be resolved in the flow, but to the cost of increased computational power. In theory a structured mesh that follows the flow pattern is the optimal solution, but unfortunately quite often not possible to achieve.

The size of the cells may be adapted to the phenomena's presented. In a large system for example it is convenient to use different restriction on the cell sizes in different areas to meet the accuracy versus computational cost limitations. Near wall region is one region that needs extra dense mesh in order to capture near wall effects. Such effects are estimated by special wall functions developed for this region, but demand a good mesh to work properly. The quality of this mesh can be judged by y+ values that should be within a certain range (Andersson et al., 2012).

A produced mesh can be judged both from density and quality point. Quality is usually measured with the assumption that the cells should be consistent, follow the stream line and not change to much from cell to cell. In (Andersson et al., 2012) is it advised to avoid highly skewed cells high aspect ratios and low squish indexes.

2.10.2 Governing equations

A generated mesh creates nodes in which various equations will be solved in an iterative manner until convergence is reached. The fluid flow is treated as a continuum and its equation of continuum is derived from various fundamental equations.

The first equation is the equation of continuity (2-31), and the second (2-32) shows the relation for the viscous stress. These equations are based on the assumption that the fluid is incompressible and Newtonian. From these combined with the Navier-Stokes equation the final equation of motion can be derived (2-32).

$$\frac{\partial U_j}{\partial x_j} = 0 \qquad 2\text{-}31$$

$$\tau_{ij} = \mu\left(\frac{\partial U_i}{\partial x_j} + \frac{\partial U_j}{\partial x_i}\right) \qquad 2\text{-}32$$

$$\frac{\partial U_i}{\partial t} + U_j\frac{\partial U_i}{\partial x_j} = -\frac{1}{\rho}\frac{\partial P}{\partial x_i} + \mu\frac{\partial}{\partial x_j}\left(\frac{\partial U_i}{\partial x_j} + \frac{\partial U_j}{\partial x_i}\right) + G_i \qquad 2\text{-}33$$

The equation of motion is a PDE that cannot be solved directly. Consequently numerical methods have to be introduced and that the flow field will be sensitive to numerical errors.

2.10.3 Numerical aspects

Many of the equations that are solved in CFD are PDEs that cannot be solved directly. These can usually be estimated by sets of algebraic equations that are solved for each cell. The choice of numerical approach here is a crucial aspect considering accuracy and stability.

For convective flows information must be transported through the system in the correct direction. To solve this issue many different methods have been created, e.g. first and second order upwind schemes. The point of using these is to calculate the face values needed to for the algebraic equations.

The first order upwind scheme uses only information of one upcoming cell, while the second order uses information from two upwind cells. This denotes that the first order is bounded and more robust compared to the second order, but is unable to reduce numerical diffusion which results in lower accuracy.

Equations solved in the simulations are usually dependent on each other. To address this coupled solvers may be used but are often to memory expensive. More common is to use different iterative methods such as SIMPLE that solves the pressure-velocity relation.

2.10.4 Convergence

Convergence is one of the most fundamental concepts for a CFD engineer. Since the systems are solved iteratively it is important to understand when the accuracy of the simulations is good enough and that they are to be considered as converged. One common way is to combine monitoring of important components, such as concentration of reactants in the outlet and monitoring of deviations in each cell (residuals). When these values go under a certain threshold criterion the accuracy is considered as good enough and the solution is converged.

The ideal situation of a steady state where the residuals goes to zero is however not always possible to reach. Sometimes fluctuations will prevail and the engineer will have to evaluate if the solution is converged and within required accuracy.

2.10.5 Turbulent modeling

Most engineering problems in today's chemical industry involve turbulent flows. Turbulence can be predicted from the Navier-Stokes equations and solved exactly. The most accurate method used today is called direct numerical solution (DNS) and gives extremely detailed information about the flow. In these simulations the fundamental equations are resolved directly for all scales. Since turbulence works at a large range of scales, varying from small to large, the computational cost quickly becomes extremely large. According to Andersson et al. (2012) cost will increase with the Reynolds number in cube, which means that DNS is not feasible for engineering problems, but only for research.

To address the computational cost many approximations have been developed throughout the years. Some are quite detailed such as the large eddy simulations (LES) that assumes equilibrium for the smallest scales, others are more rough estimations such as one equations models. The most common workhorses today (Andersson et al., 2012) are two equations models known as the k-ε and k-ω models. These are in general based on the Reynolds Averaged Navier Stokes (RANS).

2.10.6 RANS and Boussinesq

For more than 100 years ago proposed Reynolds that the instantaneous variables could be divided into an average and a fluctuating part which is illustrated below for the velocity and pressure.

$$U_i = \langle U_i \rangle + u_i \tag{2-34}$$

$$P = \langle P \rangle + p \tag{2-35}$$

By substituting these variables into the Navier Stokes equation the following equation is achieved.

$$\frac{\partial \langle U_i \rangle}{\partial t} + \langle U_j \rangle \frac{\partial \langle U_i \rangle}{\partial x} = -\frac{1}{\rho}\frac{\partial}{\partial x_j}\left[\langle P \rangle \delta_{ij} + \mu\left(\frac{\partial \langle U_i \rangle}{\partial x_j} + \frac{\partial \langle U_j \rangle}{\partial x_i}\right) - \rho\left(u_i u_j\right)\right] \tag{2-36}$$

The RANS equation (2-36) introduces Reynold stresses $\rho\left(u_i u_j\right)$ which need to be modeled to close the equation. The Reynold stresses are important to consider since they create a link between the mean velocity and the fluctuations of the velocity field. One common way to treat this term is through the Boussinesq approximation. It assumes that the Reynold stresses are proportional to the mean velocity gradient and therefore eddies behaves like molecules, turbulence is isotropic and stress and strain are in equilibrium. These assumptions indicate that models based on Boussinesq only are appropriate for isotropic flows that have local equilibrium (Andersson et al., 2012). Even though the assumption has flaws it is widely used today in many different models such as the k-ε realizable used here.

2.10.7 k-ε

The k-ε model is one of the most used turbulent models because of its relative robust and easy interpreted terms. Two transport equations needs to be solved, one for k and one for ε:

$$\frac{\partial k}{\partial t} + \langle U_j \rangle \frac{\partial k}{\partial x_j} = \nu_T \left[\left(\frac{\partial \langle U_i \rangle}{\partial x_j} + \frac{\partial \langle U_j \rangle}{\partial x_i}\right)\frac{\partial \langle U_i \rangle}{\partial x_j}\right] - \varepsilon + \frac{\partial}{\partial x_j}\left[\left(\nu + \frac{\nu_T}{\sigma_k}\right)\frac{\partial k}{\partial x_j}\right] \tag{2-37}$$

$$\frac{\partial \varepsilon}{\partial t} + \langle U_j \rangle \frac{\partial \varepsilon}{\partial x_j} = C_{\varepsilon 1}\, \nu_T \frac{\varepsilon}{k} \left[\left(\frac{\partial \langle U_i \rangle}{\partial x_j} + \frac{\partial \langle U_j \rangle}{\partial x_i}\right)\frac{\partial \langle U_i \rangle}{\partial x_j}\right] - C_{\varepsilon 2}\frac{\varepsilon^2}{k} + \frac{\partial}{\partial x_j}\left[\left(\nu + \frac{\nu_T}{\sigma_\varepsilon}\right)\frac{\partial \varepsilon}{\partial x_j}\right] \tag{2-38}$$

The closure coefficients can be chosen according to guidelines or to suit the specific situations. More details can be found in (Andersson et al., 2012). The model has some issues related to the Boussinesq approximation and other simplifications. It works poorly for low Reynolds numbers, swirls, flow separations etc. To address these issues modified versions has been created.

2.10.8 k-ε realizable

For flows with large mean strain rates the normal stresses may be negative. Another way of expressing this is that the Reynold stress tensor will not meet the Schwartz inequality for these kinds of flows. To address this issue the k-ε realizable has been developed which contains two large changes: alternative formulation of the turbulent viscosity and modification in the transport equation for the dissipation rate (ANSYS Inc., 2012). The final model can handle flow separations and swirling flow, but lacks some of the standard k-ε stability.

In order to run simulations with this model some initial data must be specified, e.g. the turbulent inlet conditions. This can be done by specifying k and ε directly or by specifying some related properties. One of these alternative properties is the turbulent intensity that describes the relation between the fluctuations and the mean velocity field. According to (Andersson et al., 2012) is the turbulent intensity normally in the range of 5-10% and can be estimated according to 2-39.

$$I = \frac{u'}{\bar{U}} = 0.16Re^{-\frac{1}{8}} \qquad 2\text{-}39$$

This together with the turbulent length scale will give the required boundary conditions for the turbulence. (Andersson et al., 2012) recommends to set this to 7% of the hydraulic length scale. From these properties k and ε may be estimated through:

$$k = \frac{3}{2}(\bar{U}I)^2 \qquad 2\text{-}40$$

$$\varepsilon = C_{\mu}^{\frac{3}{4}} \frac{k^{\frac{3}{2}}}{l} \qquad 2\text{-}41$$

2.10.9 Reactions

Achieving stable and accurate models of reactions can be challenging in CFD simulations. There are different ideas on how to incorporate these, but including detailed chemistry, transport resistances, efficiency factors etc. will soon create a complex situation that can be difficult to handle. Also finding correct numbers and models is a possible source of errors.

Modeling of reactions can be performed by including classical reaction expressions and estimate the reaction rate in each computational cell. This includes solving the transport equations for each species in order to know the exact equation. But as described in the mixing section reactions may under some conditions be regarded as pure mixing dependent. For these situations models based on a more statistical approach have been established, such as the non-premixed combustion model. In the end, the choice of reaction model and mechanisms is a question of accuracy and computational cost.

2.10.9.1 Non-premixed combustion

Under some special conditions it is possible to develop a model that solves the reactions with only one variable. This is done by simplifying the situation to a mixing problem, only

dependent on the mixture fraction. Reaction is here modeled by solving the mixture fraction in each point until equilibrium is reached.

The fundamental idea of the concept is that there are non-premixed inlets similar to Figure 3. It is important that the oxidation medium and fuel are separated in different inlets, even if the concept itself allows multiple inlets as long as all of them fulfill the non-premixed requirements.

Figure 3. The non-premixed combustion models must have two separate inlets for the oxidation medium and the fuel

To describe the situation a PDF, $\varphi(\eta)$, is created, e.g. a β-PDF or similar. From this PDF a table can be created which will be stored in a look-up table to decrease the computational costs. The table describes the conversion as a function of the mean mixture fraction and variance. From this the average concentration of the individual species can be calculated:

$$\langle c_i \rangle = \int_0^1 c_i(\eta)\varphi(\eta)d\eta \qquad 2\text{-}42$$

Details on how to model this can be found in e.g. (Andersson et al., 2012). Application of this model requires some criterions to be fulfilled such as Lewis number equal to zero, discrete fuel and oxidize inlets and they have to be of diffusional type (ANSYS Inc., 2012).

A fast reaction will be considered as a pure mixing problem (equilibrium flamelet model), since no limitations in reaction speeds will be present. The more complicated situation where there is non-equilibrium an unsteady state flamelet model will be used instead, where the kinetics of the combustion is included in the model. This can be tested by comparing relevant time scales in the Dahmköhlers number:

$$Da = \frac{reaction\ rate}{convective\ mass\ transport\ rate} \qquad 2\text{-}43$$

2.10.9.2 Species transport

To solve chemical reactions explicitly the composition must be known through the system. This can be done by solving the species transport for each individual species:

$$\frac{\partial \langle C_i \rangle}{\partial t} + U_j \frac{\partial \langle C_i \rangle}{\partial x_j} = \frac{\partial}{\partial x_j}\left[D \frac{\partial C_i}{\partial x_j}\right] + S_i(\boldsymbol{C}) \qquad 2\text{-}44$$

While the composition in each cell is known, chemical reactions can be estimated through regular reaction expressions and incorporated in the models. Such way of treating the reaction is different to the non-premixed approach since kinetics will be modeled in detail. It will be possible to treat a larger variation of situations, such as mixed inlets and slow reactions.

3 Method and setup

The general method behind this work has followed the classic engineering approach combined with modern tools. The most important tool has been the commercial software Ansys Fluent in which the CFD simulations has been performed. To be able to use this tool according to the best practices literature reviews, discussions with supervisors, data gathering and simulations has been carried out in an iterative manner.

Savings in computational cost were made by initially develop and evaluate models in 2D. To further increase the accuracy 3D simulations were implemented based on the outcome from the 2D results.

3.1 Literature review

A literature review has been carried out by using widely used internet sources. This includes Chalmers library's homepage, Google, Wikipedia, Web of knowledge, Ansys homepage etc. Information from these sources has been combined with the study of earlier course materials, and consultation with our supervisors and other people with expert knowledge. The previous study performed in the area gave crucial input needed for the project.

For information about how to use their software Ansys support has been consulted. Ansys also provides complementary information on their webpage. Their theory guide describes many methods including details and the assumptions behind it.

3.2 Data gathering

In order to simulate the process a lot of data had to be gathered. Since this project is based on an earlier master thesis much of this data was already given. Unfortunately this was not sufficient since it did not provide any catalyst data and additionally some mistakes were discovered.

To gather missing data a two day study visit to the plant located outside Palembang, Indonesia was arranged. During this visit most important data was provided and discussions with operators lead to further understanding of the reactor problem.

3.3 Software

Simulations were performed using a commercial software package from Ansys. The package consists of many different tools, of which only Workbench, Designmodeler, Meshing and Fluent were used. A short introduction to all of them follows below.

3.3.1 Workbench

Workbench connects all different tools by providing a single platform to build a complete project. In Workbench it is possible to specify some fundamental settings, such as which tools to use and 2D or 3D simulations.

3.3.2 Design modeler

The first step is to create a drawing that describes the equipment in a simplified, but realistic, way. Most difficult part for the engineer is to understand which details that is of interest and which that can be neglected. Designmodeler is the inbuilt tool in Ansys Workbench for creating these geometry models.

The 2D model was created by simply dividing the equipment into two parts, one for the burner zone and one for the catalyst zone. The inlets of the burner consist of three rows of

tubes and one perforated plate; these cannot directly be interpreted to 2D. Consequently they were simulated as four slits instead, with a width that keep the total inlet area constant.

$$W_{slit} = \frac{A_{tube\ tot}}{\pi * D_{to\ center\ of\ row}} \qquad 3\text{-}1$$

Modeling the geometry in 3D gives the possibility to create a more exact representation of the actual reactor and the rows of tubes could be modeled to correspond to reality. To minimize computational cost periodic symmetry was applied and only one fifth, a 72° segment, of the reactor volume was generated. It would be computationally favorable to simulate an even smaller segment but since gradients across periodic boundaries are zero, a larger segment was modeled to study possible angular gradients in the reactor.

3.3.3 Meshing

Generation of the mesh was done by using the inbuilt meshing software. This tool uses the geometry created in the Designmodeler and gives the engineer the possibility to set restrictions in different ways.

It can be expected that the most important mechanisms will occur close to the inlets in the burner. Thus the method “proximity” was used that will create a dense mesh close to the inlets and dilute with distance. In near wall regions inflation methods were implemented that creates a denser mesh in these areas.

When generating the 2D mesh a method was used in the catalytic zone that force all cells to be quadrilateral. In 3D a sweep function was used in the catalyst zone mesh that simply creates a 2D mesh in one edge and then extrudes it into a 3D mesh resulting in a more structured mesh.

3.3.4 Fluent

In fluent the mesh is imported and simulated to solve the fundamental equations in each of the computational cells. It also allows including many different types of mechanisms, including reaction, heat transport etc.

The main strategy has been to start simple and in an iterative manner include more mechanisms and more advanced models. This can be seen in the result part where different methods have been compared in order to find out where the limitations can be found. Some models choices could however be established prior to the initial simulation.

Turbulent model of choice was the k-ε realizable, since it can handle swirling flows that can be expected and still give a reasonable computational time. Since k-ε cannot handle low Reynolds number it is not appropriate close to walls, where a wall function was implemented instead. A non-equilibrium wall function was selected due to the suitability for swirling and flow separations.

The catalytic bed was treated as a porous zone. Inertial and viscous resistance parameters were first estimated by help of (2-10) and (2-11) and later on optimized to achieve the real pressure drops. Flow through the porous zone was considered turbulent and radial dispersion was neglected (see result chapter).

Inlet conditions were set according to process data. This includes composition, pressure, temperature etcetera (see Appendix: Setup simulations for more information). Turbulent intensity and hydraulic length scales were estimated and set according to the theory chapter.

Reaction in the burner was modeled as non-premixed combustion with non-adiabatic settings. The choice can be motivated with that this method has been proven to work well for this kind of combustion process and is in fact a standard tool today.

Catalytic reactions cannot use the same concept and were modeled with a species transport approach instead. This general method is unfortunately not compatible with the special non-premixed model and therefore had to be simulated separately. This was done by simulating the whole reformer reactor with an inert catalyst, just including combustion reactors. A profile over the flow data was copied at the boundary between the burner and the catalyst and used as inlet condition in the second simulation, where the catalytic reactions were simulated.

The reactions in the catalyst were specified in a UDF (see below). The implementation of the UDF was done through a source term for the flow and not as a specific reaction. To be able to model the heat transfer resistance the porous bed split into two parts, one solid and one fluid. Between them heat was transported which was modeled through a heat transfer coefficient defined in the UDF. Heat of reaction was also included in the UDF and was set to be consumed on the catalyst surface.

Mass transport resistance was originally modeled specifically for each species. But after convergence problems and the limited time frame a constant global efficiency factor was implemented instead. This efficiency factor was corrected to fit real process data and was included in the UDF as limitation on the reactions rate expressions.

3.3.5 UDF

Fluent allows the engineer to include custom made code in the simulations. This code can include specifications for inlet conditions, reactions, heat transfer coefficients etc. In this project the catalytic reactions, heat transfer coefficient and heat of reaction were modeled in such manners. This implementation has been performed by the use of source terms.

The UDF can be found in Appendix: UDF and consists of in total six functions. The approach for the code is that it will use the data in the computational cell it is evaluated in, in order to calculate the required property. The code is written in C, which is one of the standard languages in the modern computer science.

4 Results

4.1 Calculation of Adiabatic burner

To study if the issues observed in the reactor could be connected to hot spots a simple calculation of maximum flame temperature was done. In the calculations perfect combustion was assumed. By using the composition of process data a maximum temperature of 1372K was reached.

The estimated temperature is lower than the temperature that is specified in the material specification for the refractory bricks and should not give raise to any issues. This primary calculation however indicates nothing about the distribution of the heat in the reformer and just the maximum reachable temperature assuming an adiabatic flame.

4.2 Equilibrium flamelet

In order to decide if the equilibrium flamelet approach could be used in the non-premixed model some calculations were performed. The Dahmköhlers number (2-43) was estimated for the combustion reactions by the end of the burner zone. Combustion reaction rate constants were taken from (Warnatz, 1981) where the chemistry of hydrogen and methane combustion consisted of 21 steps. The relevant time scale for reaction was estimated by assuming second order reaction and extracting species concentration from Fluent at the end of the combustion zone. It is possible that the estimated values of Da are slightly underestimated due to the assumption of second order reaction.

Calculations show that only a few of the reactions have Dahmköhler numbers close or above unity while most have very low value. Reactions with low Damköhler values indicate that these have reached equilibrium and the reaction has practically stopped which would verify that they are very fast reactions. Both consumption of methane and hydrogen, which are the reactions of most importance in this case, show such tendency.

Reactions forming oxygen from HO_2 are the only ones with Damköhler number values above unity. This indicates that these reactions have not reached equilibrium. Since these reactions are not critical in our simulations and due to the occurrence of alternative reaction paths to form oxygen the equilibrium flamelet approach was considered valid. The low concentrations of radicals and reagents observed in Fluent also support this idea.

4.3 2D simulations

Some 2D simulations were carried out to develop a model for the reactor. This was done by testing different modeling aspects individually in an iterative manner.

4.3.1 Geometry

Two different geometries were created, one for the whole reformer and one for the catalytic zone only. The air inlet tubes were treated as slits and the dimensions were chosen according to given drawings and information attained during the study visit.

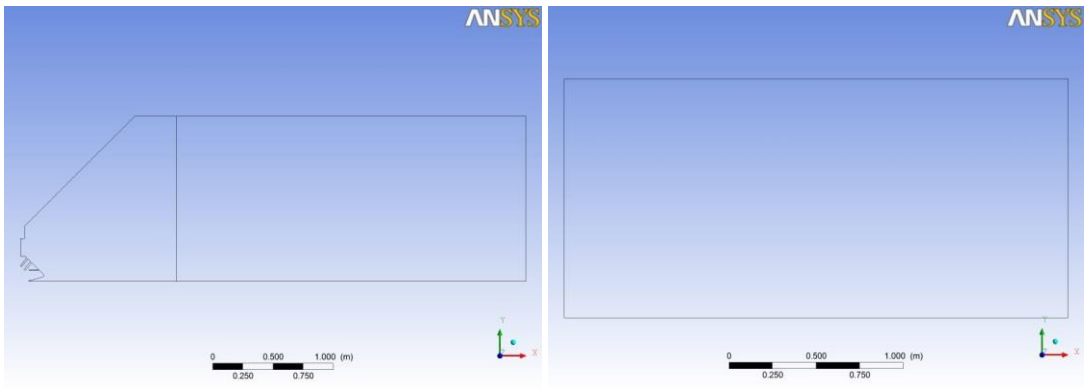

Figure 4. Geometry of the reformer and the catalyst.

4.3.2 Pressure drop

The drop in pressure in the reactor is related to the porous catalyst bed. Model coefficients were estimated through equation 2-10 and 2-11 and then optimized by changing them relatively to each other until the pressure drop correspond to real process data. Final coefficient used were 3 813 000 for viscous resistance and 4 176 for the inertial resistance. This gives a pressure drop of 0.32 bar, which is in the same range as the process data.

4.3.3 Mesh independency

The first step was to create a grid that was reasonably mesh independent, but still coarse enough to keep the computational cost low. Three different meshes were created for the standard case, containing 20 000, 30 000 and 40 000 computational cells. Converged solutions of the three meshes were further compared in global and local variables. Temperature profiles and difference plots can be seen in Figure 5 and Figure 6 for the comparison cases 20k vs 30k and 30k vs 40k.

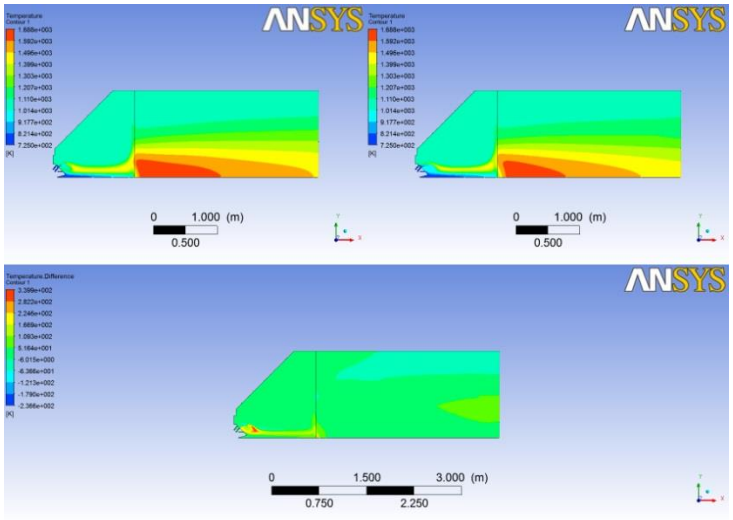

Figure 5. Comparison between 20k and 30k

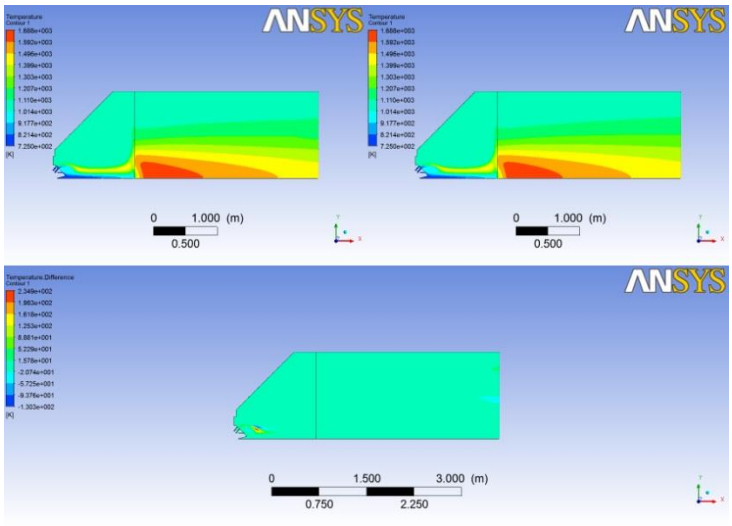

Figure 6. Comparison between 30k and 40k

In the first case 20k vs 30k the differences are small but still significant. Even in the case 30k vs 40k there are some differences, mostly focused to a few points. To see how this influenced the outcome some variables were monitored:

Table 3. Comparison between different density of the mesh. The data is taken as an average value at the outlet.

case	Mass flow [kg/s]	Temperature [K]	Velocity [m]
20k	28.34	1154.6	0.992
30k	28.34	1159.1	0.993
40k	28.34	1159.7	0.992
20k with laminar	28.34	1161.1	0.992

It can be seen that the differences are quite small. A decision was taken to use the case 30k since no large changes was to be found when increasing the number of cells to 40k. Another reason to use the 30k mesh was lesser computational cost. Figure 7 depicts the final mesh in 2D.The mesh quality do not meet all of the requirements in the best practice guidelines (Andersson et al., 2012). But since the 2D simulations only are used for development of the model, this level of quality was accepted. Efforts were also put in to keep the y+ values close to the walls according recommendations.

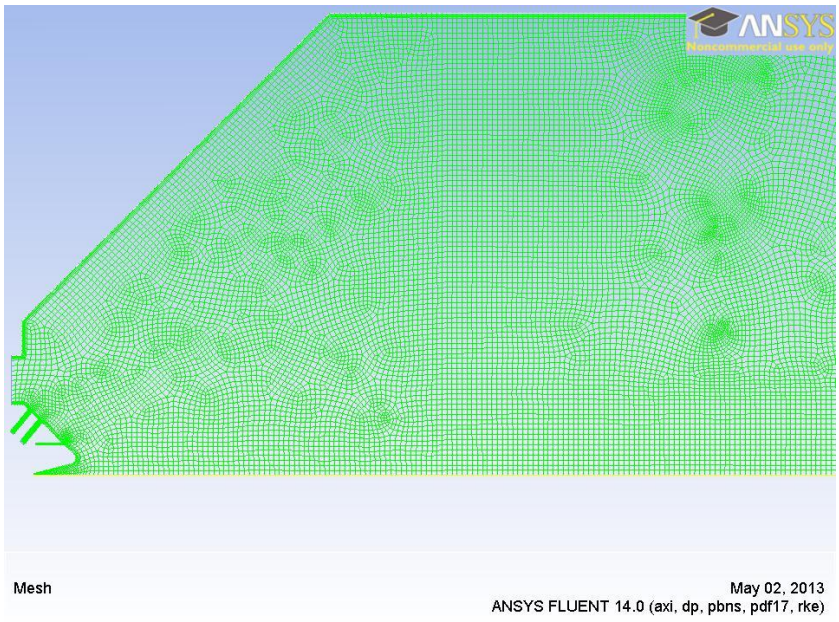

Figure 7. The final mesh, only a part of the catalyst is shown here.

4.3.4 Turbulent vs. laminar

For high Reynolds numbers turbulence will be prevalent in the flow. In the inlet region of the burner turbulence will be of importance for the flow characteristics and therefore also the mixing. For packed beds this is however not always true and therefore two simulations were obtained that compares turbulent and laminar treatment of the packed bed. The comparison is illustrated in Figure 8 by the resulting temperatures.

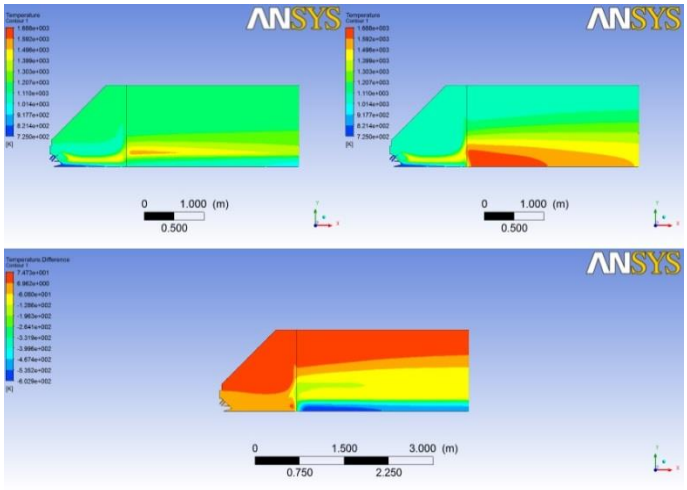

Figure 8. Comparison between laminar and turbulent flows, temperature.

The comparison plot shows large deviation for the two cases. An estimation of the Reynolds number through the packed bed gives a value of about 5000 (using an equivalent particle diameter of 2.4cm), which indicates a fully turbulent flow. From these findings it was decided to treat catalytic bed as a turbulent region.

4.3.5 First and secondary upwind scheme

The first order upwind scheme has some issues with numerical diffusion. To see if this was true for this case a comparison plot with first and second order upwind schemes was produced:

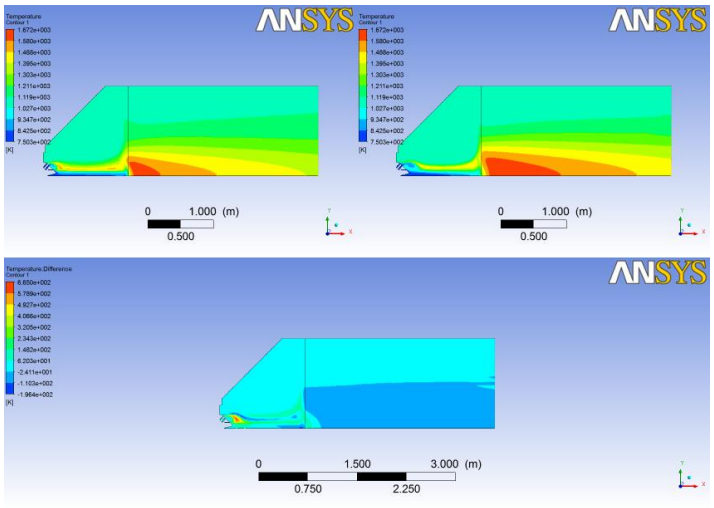

Figure 9. First vs second order upwind scheme

As can be seen in Figure 9 there are evidently quite large differences. Thus it is safe to say that numerical diffusion is a significant source of errors and second upwind scheme should be used.

4.3.6 Inlet properties

Inlet conditions were specified through estimated turbulent intensities and turbulent length scales. To see how these influenced the outcome a series of tests were carried out varying turbulent properties. Test setup and results can be seen below:

Table 4. Test setup for inlet conditions

Case	Parameter	Change	Where	Average temperature at catalyst surface [°C]
A	Standard case			1155
B	Turbulent intensity	+100%	Air inlet	1156
C		-50%		1154
D	Hydraulic diameter	+100%		1157
E		-50%		1154
F	Turbulent intensity	+100%	Gas inlet	1155
G		-50%		1156
H	Hydraulic diameter	+100%		1155
I		-50%		1155

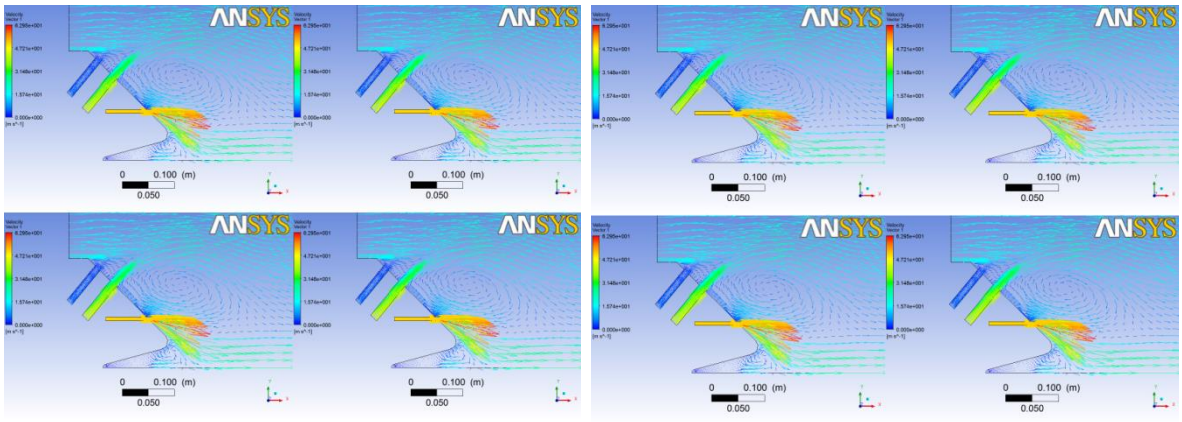

Figure 10. Velocity vectors for the change in inlet properties. The different cases follow Table 4 with A in the upper left corner.

As can be gathered from Table 4 and Figure 10 the outcome will not change significantly when overestimating or underestimating turbulent intensities and length scales. Both air and gas inlet conditions were studied in this analysis.

The gas inlet is equipped with perforated plate across the pipe. There are different approaches to model this but here the turbulent intensity has been considered to survive the perforated plate. This decision was based on the fact that it takes some times for turbulence to develop through a system. An engineering rule says that the length of a system needs to be about ten times the diameter to develop a fully turbulent flow (Cairo University, 2006). The hydraulic diameter was chosen according to the diameter at the perforation holes. To test the influence of this condition a simulation was ran assuming the gas inlet had no perforated plate. This mean increasing the hydraulic diameter to the actual pipe size.

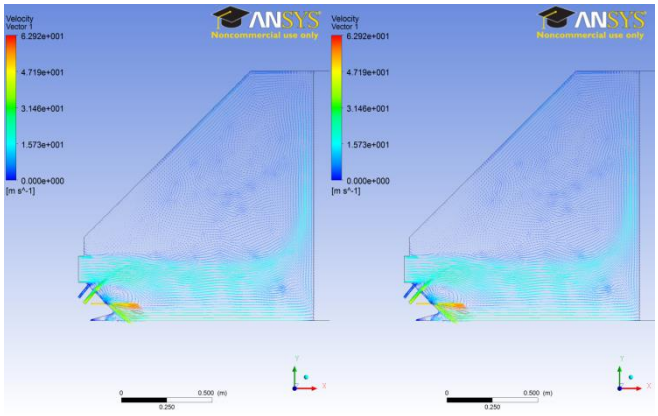

Figure 11. Simulation without any perforated plate at the gas inlet.

From Figure 11 it is clear that the flow pattern does not change significantly. Also the extent of reaction did not change which can be illustrated with an average temperature of 1155 which is in the same range as all other tests performed (see Table 4). Gathered results indicate that the solution is quite insensitive to changes in the boundary conditions at this operating point.

4.3.7 Adiabatic and non-adiabatic extensions of non-premixed model

Fluent gives the opportunity to extend the simulations using the non-premixed model with a non-adiabatic feature. Temperature plots for the standard case using adiabatic and non-

adiabatic combustion settings and a difference plots between the two can be observed in Figure 12.

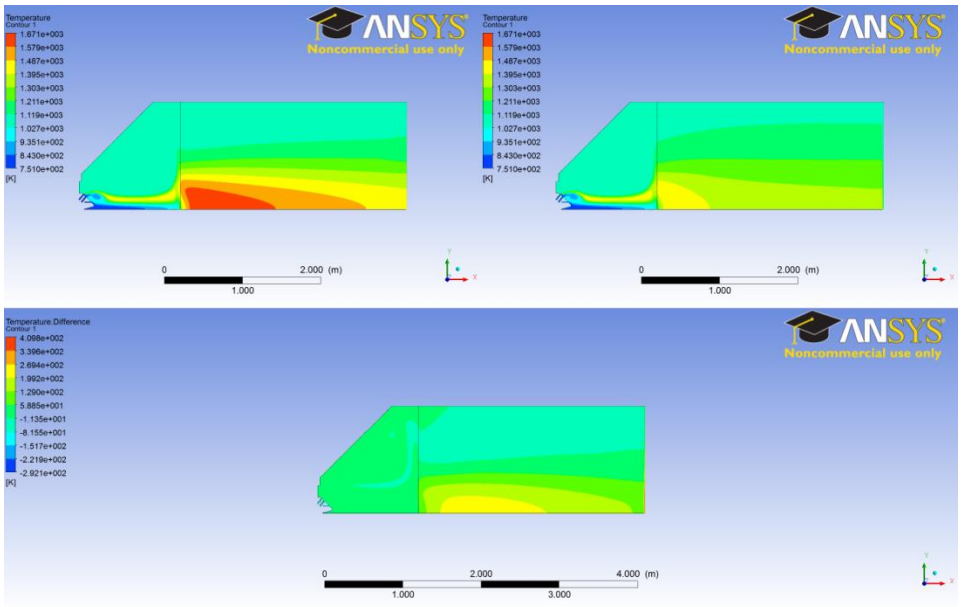

Figure 12. Adiabatic (left) versus non-adiabatic (right) extension of the non-premixed model

As expected are there no large differences in the burner but there are some significant changes in the catalytic zone. Having the peak temperature after the burner zone inside the catalytic zone might be connected to both reactions and thermodynamic properties. No deep analysis will be included about that here, since the catalyst will be simulated separately and is of secondary interest.

Results indicate that adiabatic combustion setting can fulfill the requirements for simulating the burner. However, to give the opportunity to later on include heat losses through walls, radiation and also include steam reforming reactions it would be more convenient to use the non-adiabatic approach.

4.3.8 The catalyst bed

Since the non-premixed combustion model does not easily accept the implementation of user defined reactions the catalyst had to be simulated separately. Catalyst bed inlet conditions were copied from whole reformer simulations with inert catalytic bed. The profile was extracted one cell into the catalytic bed to avoid effects from possible interface issues. Reactions were modeled using a UDF, which included a global efficiency factor for the mass transport resistance.

Table 5. Outcome of 2D simulation of the catalyst compared to real process data.

Species	Mole fraction simulation	Mole fraction real
CO	13.3	11.9
CO2	8.8	8.6
CH4	0.6	0.6
H2	58.5	56.5
H2O	0	-
N2	18.7	22.2

Product composition corresponds quite well to reality according to Table 5. The process data fluctuates and values above should therefore only be seen as guidelines. In Figure 13 the mass fraction of methane over the catalyst can be observed. As expected it decreases through the system.

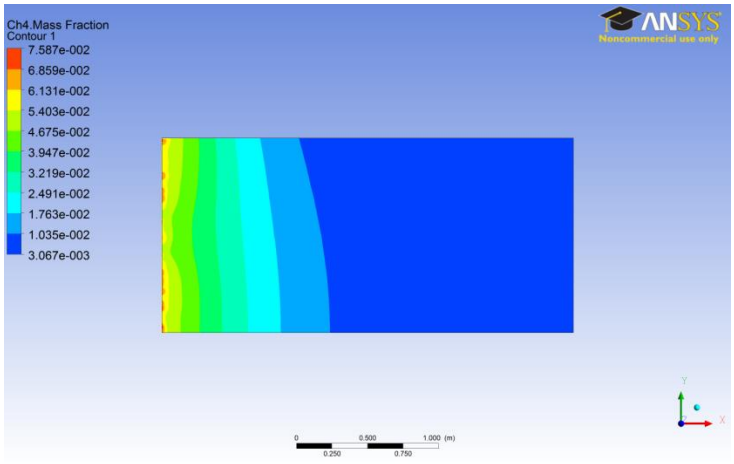

Figure 13. Mass fraction of methane across the catalyst

4.3.9 Mechanical radial dispersion

In the catalytic bed the fluid will not move freely since it will be influenced by the physical blocks that the catalyst give raise to. The importance of this was tested by implementing a radial dispersion in Fluent according to (2-13). It can be expected to give largest differences in simulations of the laminar case, since turbulence already will give random movements in the radial direction. The results can be seen in Figure 14.

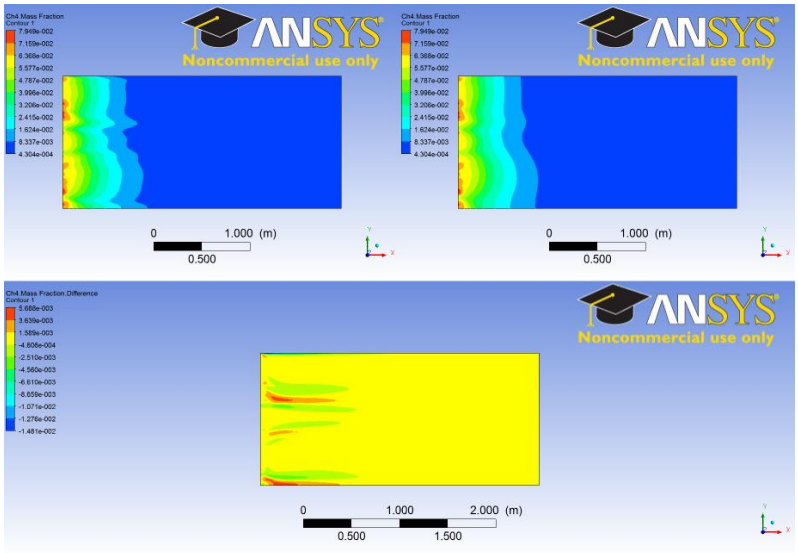

Figure 14. Comparison for a laminar flow with and without taking into account the radial dispersion in radial direction

As can be seen there are differences where the radial dispersion will give a smoother distribution. For the turbulent case this effect is already present and the differences will be even smaller. Consequently radial dispersion should be negligible in our simulations.

To support this assumption two relevant time scales were estimated (2-14) and (2-15). These calculations gave a radial dispersion timescale of 500 s and an axial transport of about 2 s.

They are clearly magnitudes in difference and thus assuming that radial dispersion has insignificant effect on the final solution is valid.

Results 3D

Setting and models evaluated in 2D were implemented in 3D simulations to study the flow pattern and temperature and concentration profiles over the reactor. These simulations are far more representative to the real case and a more qualified analysis can be carried out. In 3D has only simulations with burner combined with an inert bed been simulated.

4.3.10 Geometry

The produced 3D geometry model comprise one fifth of the total reactor. Figure 15 below illustrates the reactor geometry and a detail view over the burner inlet.

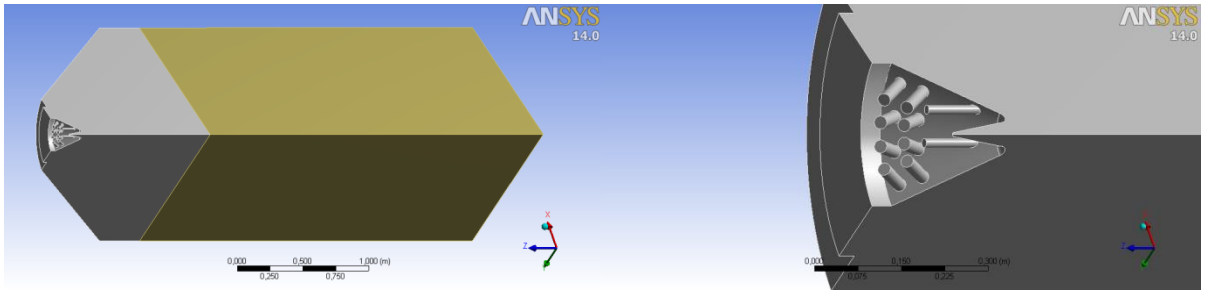

Figure 15. Geometry model of complete reactor (left) and burner detail (right)

4.3.11 Mesh independence

In order to produce a mesh independent 3D solution a set of three different meshes with varying number of elements were simulated, presented in Table 6. Converged solutions of the three cases were analyzed by comparison to determine acceptable mesh independence. Table 6 also includes monitored values of area-average temperature and velocity over the catalyst surface inlet.

Table 6. Number of elements and average temperature and velocity at the catalyst inlet for mesh 1,2 and 3

Mesh	Number of elements	Average temperature [K]	Average velocity [m/s]
1	200 000	1194.13	7.6682
2	440 000	1195.59	6.9437
3	624 000	1195.83	7.2072

As can be seen from the table the average temperatures and velocities do not change very much with improved mesh, but further mesh independence analysis is required for better local accuracy.

Temperature contour plots for simulations using mesh 1 and mesh 2 are shown in Figure 16 and Figure 17, showing different views of the geometry. The figures also depict a comparison plot (right) where the difference in temperature profile in mesh 1 and mesh 2 is observable.

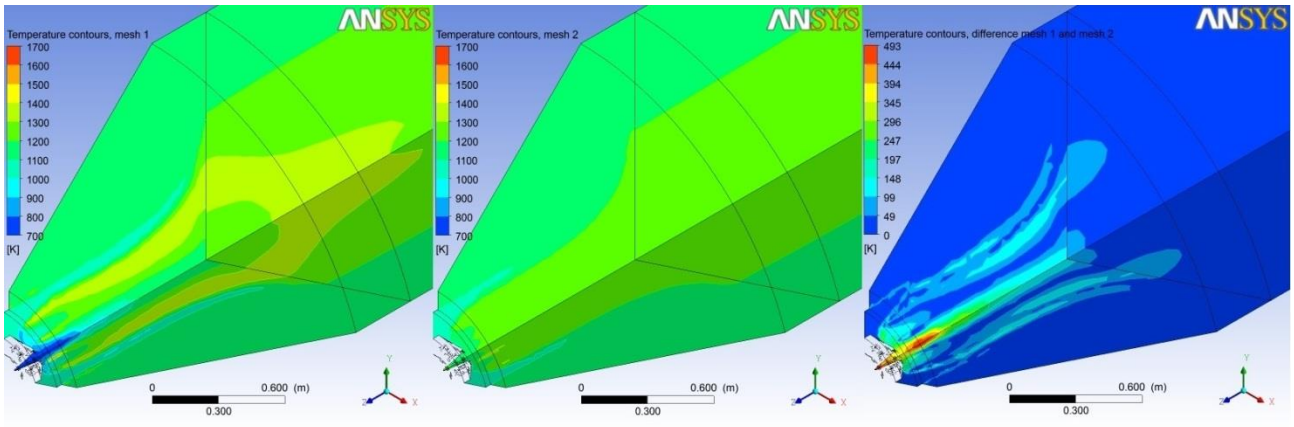

Figure 16. Temperature contour plots over the reactor burner. From left to right: mesh 1, mesh 2 and a difference plot

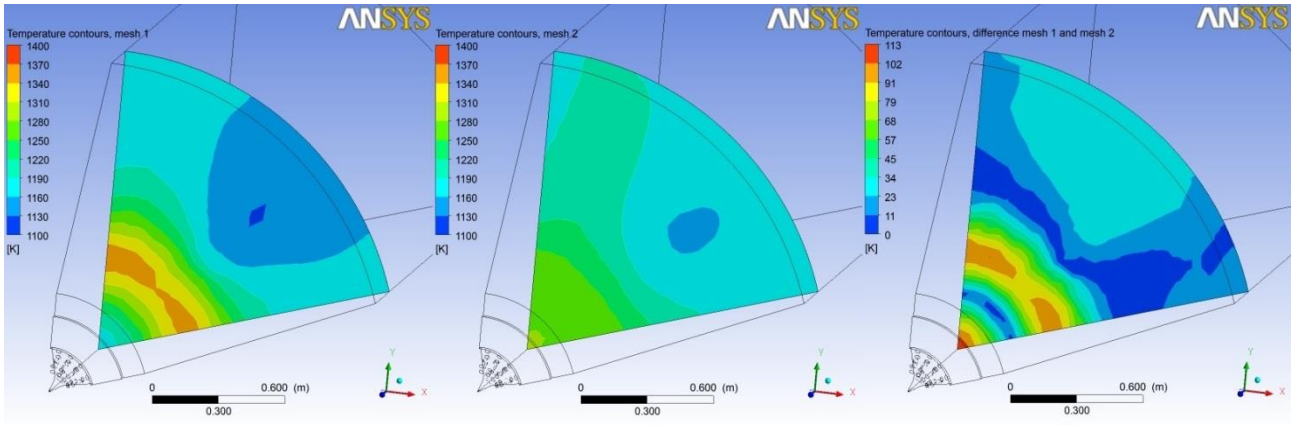

Figure 17. Temperature contour plots over the catalyst surface. From left to right: mesh 1, mesh 2 and a difference plot

The difference plots clearly show large differences between the solutions for mesh 1 and mesh 2. Thus, revealing that the solution changes significantly with mesh 2 in comparison with the initial mesh, indicating that simulations with mesh 1 are not reasonably mesh independent.

The comparison plots between mesh 2 and mesh 3 are shown in Figure 18 and Figure 19. The difference plot is presented here too.

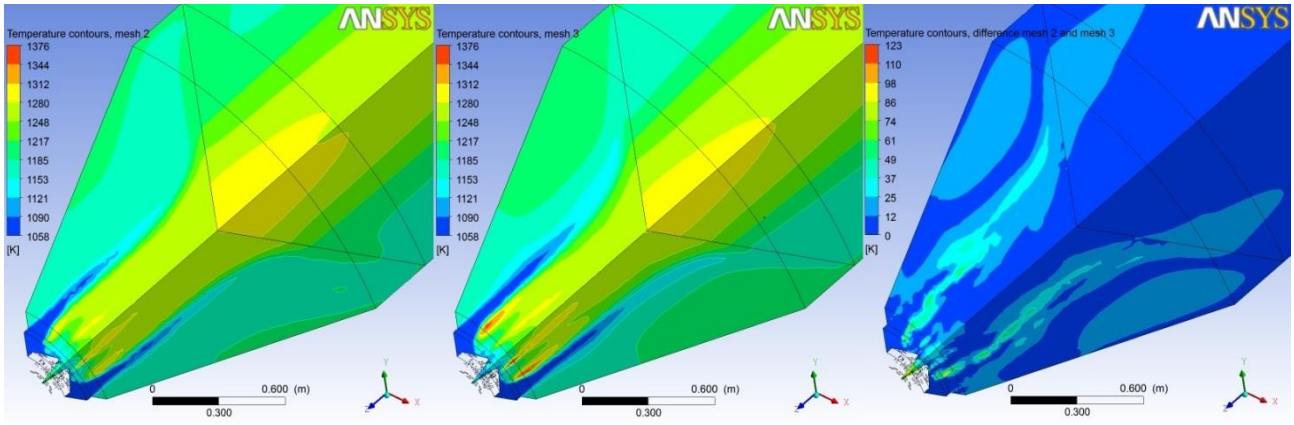

Figure 18. Temperature contour plots over the reactor burner. From left to right: mesh 2, mesh 3 and a difference plot

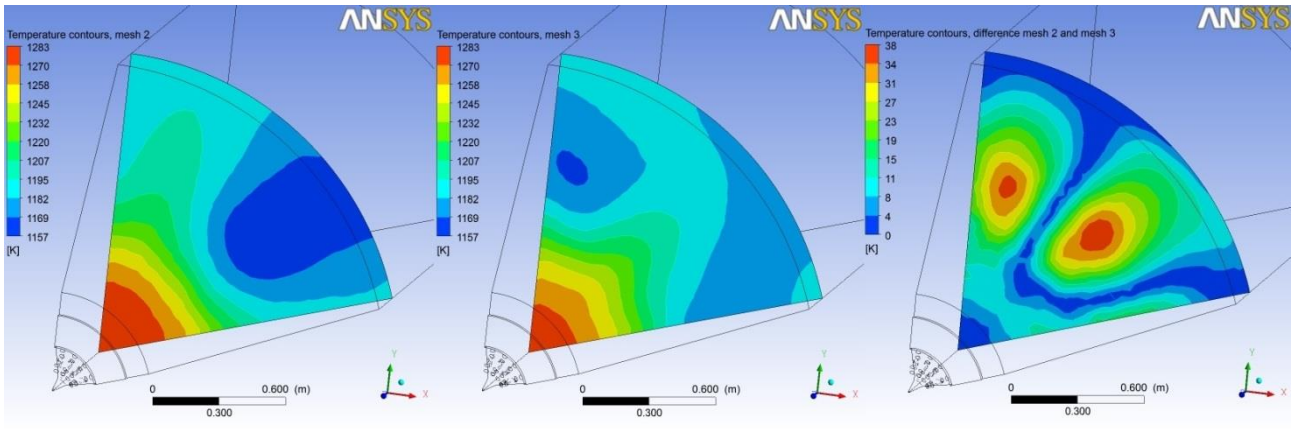

Figure 19. Temperature contour plots over the catalyst surface. From left to right: mesh 2, mesh 3 and a difference plot

From figure observations it can be seen that the solution changed marginally with the improved mesh 3 with few large local differences. But the solution differences can be regarded as insignificant and thus sufficient mesh independence is obtained for simulations performed with mesh 2.

4.3.12 Standard case

A standard case was initially simulated to represent the real reactor and to illustrate the actual problem. Later simulations use this standard case as a reference for comparison. Table 7 contains extracted area-averaged temperature and methane mass fraction at the catalyst surface.

Table 7. Data for standard case simulations in 3D.

Average inlet catalyst surface temperature (K)	**Average inlet catalyst surface CH_4 mass fraction**
1198	0.05965

Subsequently a series of contour plots showing mean mixture fraction, temperature, velocity and pressure for the standard case are gathered in Figure 20.

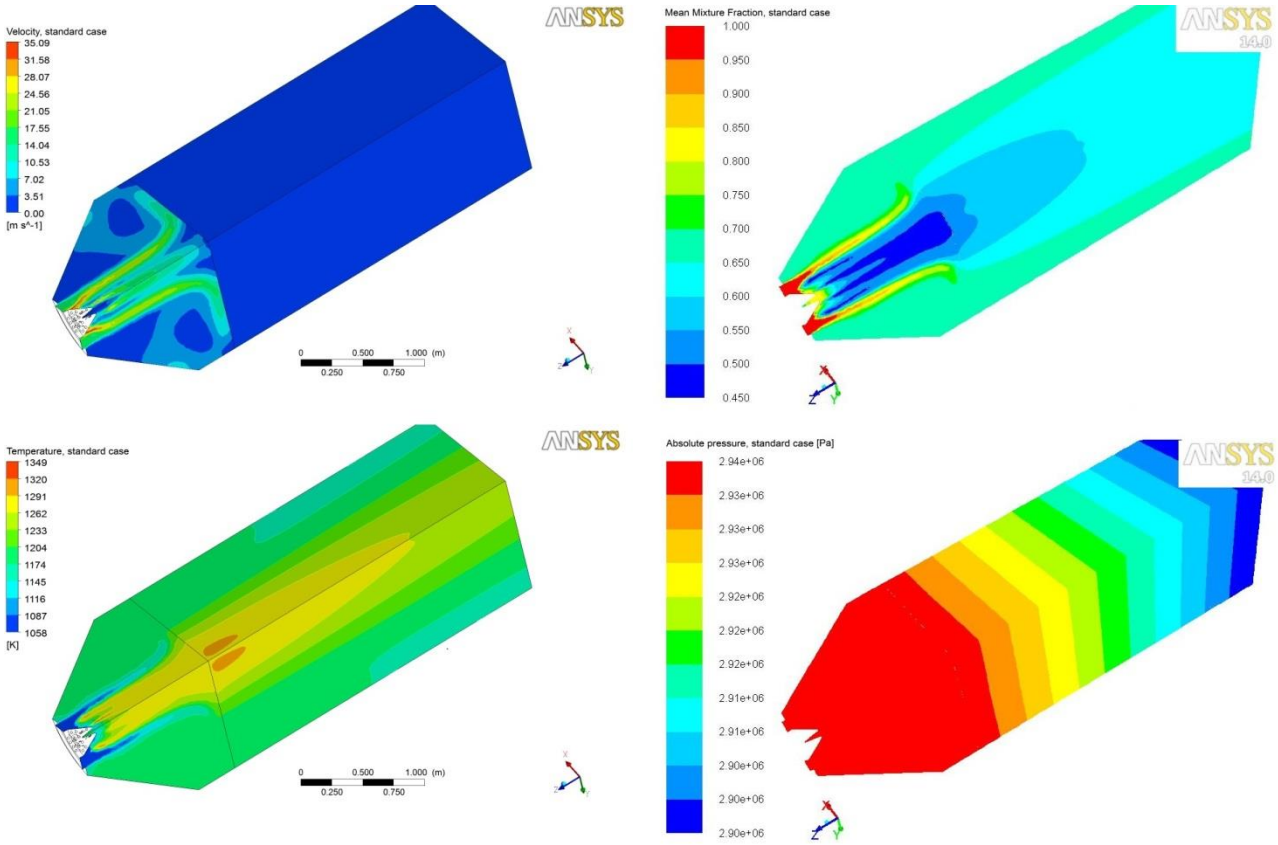

Figure 20.Variety of contour plots for the standard case. Clockwise from upper left: velocity, mean mixture fraction, absolute pressure and temperature.

The selected settings to recreate the reactor pressure drop give satisfactory result also for 3D simulations. Both the temperature and the mean mixture fraction clearly indicate an uneven cross sectional distribution. An understanding of underlying factors to this can be gathered from the velocity contours over the burner. Both the process gas and the air flow enter the reactor at high speed practically parallel to one another which leaves little room for efficient mixing. As the reactants hit the catalyst bed surface right on an impinging flow situation arises.

The heat of reaction is illustrated in detail in Figure 21 where temperature and mixture fraction variance near the burner can be observed.

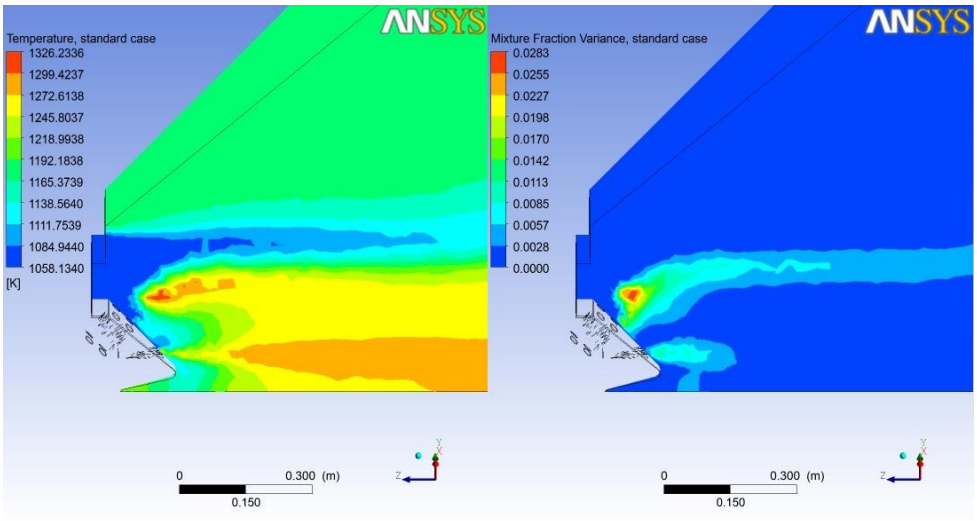

Figure 21. Detail burner view showing temperature contours (left) and mixture fraction variance contours (right)

Mixture fraction variance indicates where the fuel and oxidizer is mixed and thus where the combustion reaction occurs. As the heat is released the temperature increases as can be seen in the temperature plot which correspond well to the points of increased mixture fraction variance.

To study the flow pattern in detail the streamlines are shown in Figure 22 below.

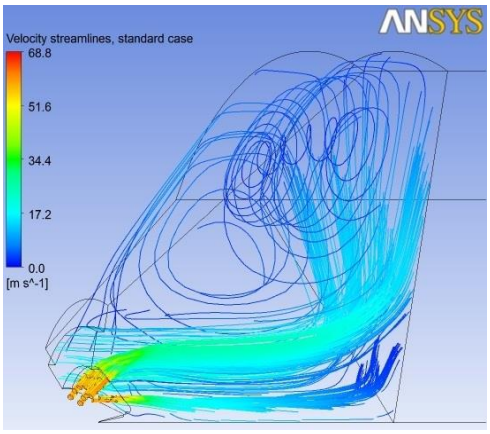

Figure 22. Streamlines plot over the combustion zone

The initial remark is here verified where the impingement of the gases is apparent. Another important observation is the recycling flow arising at the vessel walls.

4.3.13 Air inlet sensitivity analysis

To study how the flow pattern and temperature distribution changes when varying mass flow through the inner, middle and outer rows of air inlet nozzles a sensitivity analysis is carried out with a total of 6 different simulations performed.

Simulations 1-3 were carried out changing each single row one at a time according to Table 8. The original total air mass flow was kept by lowering the mass flows of the remaining air tube rows. To complement the analysis, area-weighted values of methane mass fractions and temperature at the catalyst surface were extracted.

Table 8. Air inlet mass flow change simulations 1-3 with extracted average temperatures and methane mass fraction

Simulation	Air inlet tube row	Change	Average inlet catalyst surface temperature (K)	Average inlet catalyst surface CH_4 mass fraction
1	inner	+20%	1199	0.0599
2	middle	+20%	1200	0.0598
3	outer	+20%	1197	0.0590

Temperatures and methane mass fractions are close to identical for the different cases. This indicates that the extent of reacted methane hardly will be influenced by changes in mass flow rates of the air inlets.

The influence on reactor temperature profiles from varying mass flow distributions is shown by the temperature contours of the across the catalyst surface, plotted in Figure 23 for the first 3 simulations.

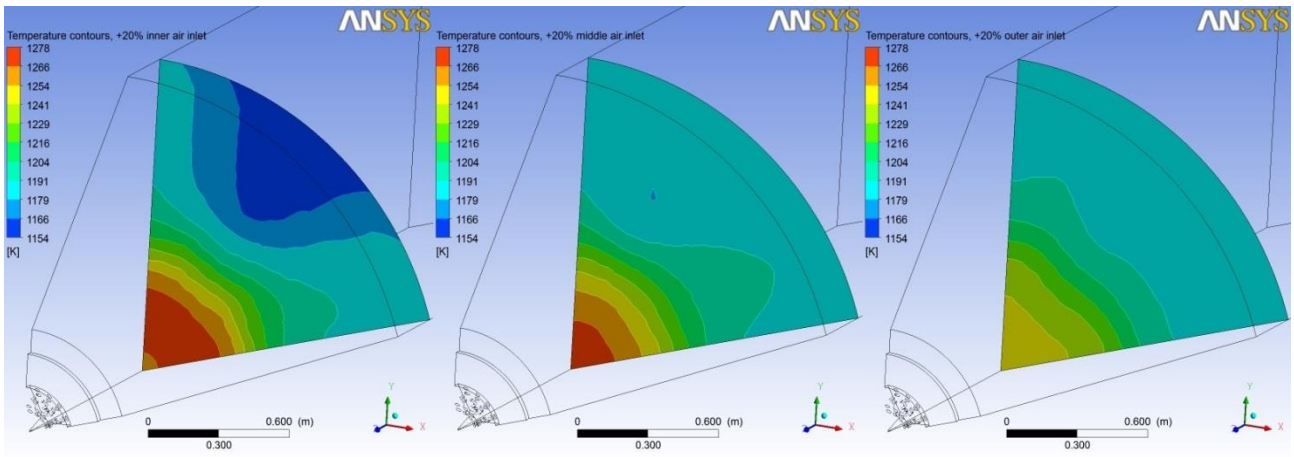

Figure 23.Temperature contour plots over the catalyst surface. Left to right: simulation 1,2 and 3

It is evident that changes in the air inlet row distribution will affect the temperature profile at the catalyst surface. A more even temperature distribution is achieved when increasing the mass flow of the outer tube row. The methane concentration profile into the catalyst also follows the same trend as the temperature profile (see Figure 29, Appendix: Air inlet sensitivity analysis; mean mixture fraction), that is, more evenly distributed as the outer air inlet mass flows are changed.

The resulting flow pattern for the varying air inlet mass flows is shown as streamlines colored by velocity magnitude in Figure 24.

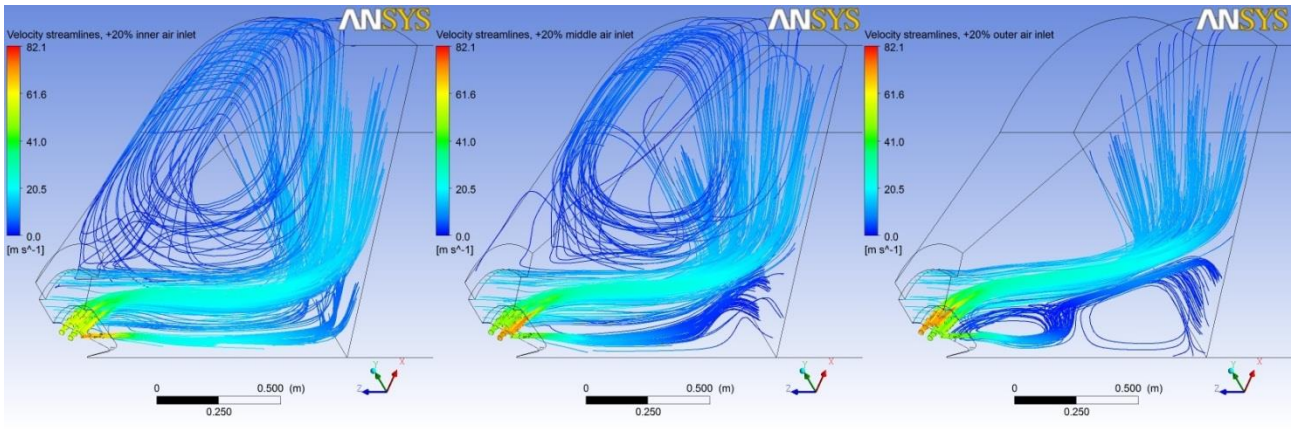

Figure 24. Streamlines plots over burner zone. Left to right: simulation 1,2 and 3

When manipulating the inner air inlet row the large gas stream freely flows in a straight line causing a strong impinging flow situation as it hits the catalyst surface, much like the standard case. However, if the outer row air mass flow is increased the flow picture is significantly changed. Most notable is the recirculating flow arising in the center part of the combustion area and the way the air flow streams into the gas flow in an angle of attack.

An additional temperature contour plot over the combustion zone can be seen in Figure 25.

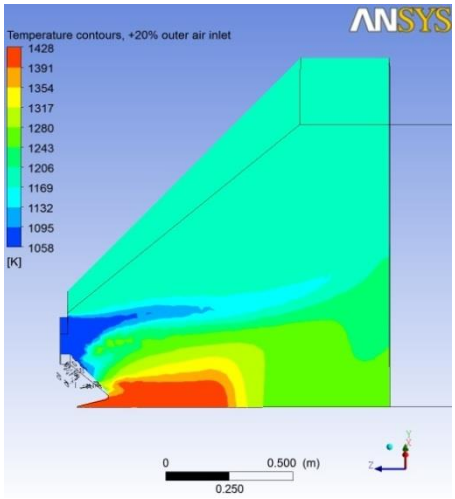

Figure 25. Temperature contour plot over burner for the simulation with + 20% air mass flow in the outer row.

There is a local high temperature region located near the burner. This is thought to arise due to the recycling flow that could be observed in the previous Figure 24.

Remaining stimulations in the sensitivity analysis features increased mass flows in 2 rows according to Table 9, showing simulation 4-6 with corresponding area-weighted temperature and methane mass fractions at the catalyst surface. Like in the previous runs, the remaining air inlet is adjusted to keep the total air flow.

Table 9. Air inlet mass flow simulations 4-6 with extracted average temperatures and methane mass fraction

Simulation	**Air inlet tube row**	**Change**	**Average inlet catalyst surface temperature (K)**	**Average inlet catalyst surface CH_4 mass fraction**
4	inner+middle	+20%	1198	0.05975
5	inner+outer	+20%	1200	0.05973

6	middle+outer	+10%	1195	0.05962

Just as in the first three simulations, the average temperature and methane concentrations remain practically unchanged.

Temperature contours for simulations 4-6 are shown in Figure 26 below.

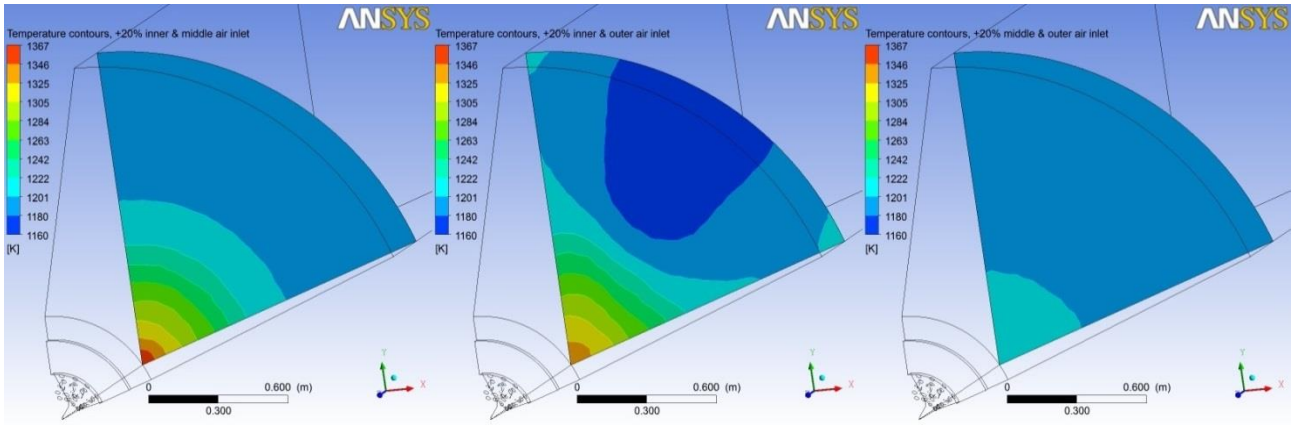

Figure 26. Temperature contour plots over the catalyst surface. Left to right: simulation 4,5 and 6

A similar trend as in simulations 1-3 can be observed where a more even temperature distribution is achieved for increased outer and middle air inlet mass flows. The concentration profile across the catalyst surface shows the same tendency (see Figure 30,Appendix: Air inlet sensitivity analysis; mean mixture fraction).

The flow pattern is illustrated by streamline plots presented in Figure 27.

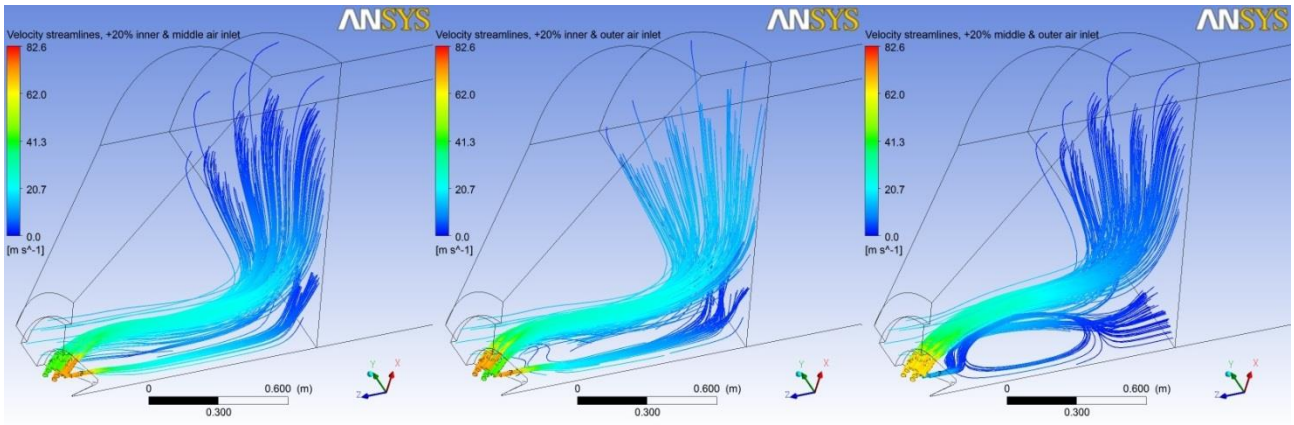

Figure 27. Temperature contour plots over the combustion zone. Left to right: simulation 4,5 and 6

Once again a similar flow field as in the single air inlet manipulation simulations can be observed. As the mass flow is increased in the outer rows, a recirculating flow is observed in the central regions of the combustion zone.

5 Discussion/Analysis

5.1 Accuracy of simulations

The reliability of the CFD simulations that were carried out must be evaluated. Important factors influencing the solution accuracy are grid resolution and quality, model selection, boundary conditions and convergence criterions.

An adequate mesh is one of the most challenging parts to model. In 2D problems were encountered when attempting to create a structured mesh in the catalytic zone and could not be achieved. This indicates mesh quality deviating from optimal standards. However, the 2D simulations were reasonably mesh independent and increased grid resolution would not give significant changes in solution. In 3D the catalytic zone was successfully meshed in a structured manner, achieving better quality. As for mesh independence in 3D, consideration for high computational cost for simulations with large number of elements had to be taken. When establishing the final 3D mesh some changes in improved mesh solutions could still be observed, but they were measured to be in acceptable ranges and the solution was considered reasonably independent of the grid resolution. In both 2D and 3D near wall effects were accounted for by implementing inflation methods giving satisfactory y+ values. Overall the mesh quality is considered acceptable, but it should also be regarded as one of the most important factors for introducing errors to the solution.

A mesh will always give raise to some extent of numerical diffusion which becomes less influent with increased grid resolution. Since our solutions are not perfectly mesh independent, it is probable that numerical diffusion affects the solution. However, the extent of it is also minimized by the use of second order upwind discretization scheme, which are proven to be less diffusive than the first order equivalent. Hence, numerical diffusion can be considered established but will not severely affect the reliability of the simulation results.

Choice of boundary conditions at the reactor inlets were estimated through commonly used guidelines. The sensitivity analysis of the inlet conditions shows that there are no significant changes in solution when over- and underestimating of turbulent properties. The results are from 2D simulations and since the deviations are close to zero, the same analysis in 3D will probably give similar result.

The use of periodic boundaries can be a source of errors. It cannot be neglected that the effects in angular direction can be connected to the use of these conditions. This can be investigated further by simulating a larger section of the catalyst, but has not been done here due to the limited time frame. The effect is however mainly found in the region close to the walls of the reactor, a region where the reaction rate is low. This would therefore only have a small influence on the conclusions for this work.

Implemented models in our simulations were selected according to best practice guidelines and consequently evaluated. However, the reality is always more complicated than the models that attempts to describe it but they can be considered to reach satisfactory accuracy. The in-built models and our developed UDF are based on many assumptions that will be discussed here.

The choice of using k-ε realizable turbulence model can be considered an appropriate choice since it suits our flow situation well. The same conclusion can be drawn by the use of non-equilibrium wall functions that can handle flow separations and impinging flows.

Modeling the combustion reactions with non-premixed combustion is partly motivated by the estimations of the characteristic equilibrium time for the flame. The method is a common way to estimate these fast reactions and usually gives reasonable results. The result can however not be verified, since no data is available in the burner.

One important phenomenon that was left out is the radiation. The radiation would here increase the heat transport, both in the burner and in the catalyst. In the catalyst this would lead to a warmer surface which in turn would lead to a faster reaction. In the flame the maximum temperature would decrease, but since the gas absorbs radiated heat the average temperature would remain quite constant but more evenly distributed.

The reactor has also been simulated as an adiabatic reactor. In reality the tower is cooled by a water-jacket and there are significant heat losses from the walls. These losses would decrease the temperature close to the wall, but since the gas flow rate is high it would not have severe effect on the methane conversion.

Considering the absence of radiation and assuming an adiabatic reactor it is clear that the simulations in terms of heat transport do not correspond satisfactory to the reality. But through the above discussion and understanding of the effects the results are still gives important indications. Radiation will increase the heat flux through the gas to the solid surface. Therefore might the reaction rate increase slightly, but the importance

Finally the UDF describing the catalytic reactions is the most significant factor for introducing errors in the catalyst simulations. The mass transport limitation is simplified by use of a fixed global efficiency factor. This means that local effects from temperature, individual species etc. can introduce errors. On the other hand gives this a good overall estimation that can be verified against real plant data. It is important to remember that he UDF only is used in simulations that are of minor interest for the main problem formulations.

To achieved converged results in 2D did not lead to any large issues. In 3D was this harder since the complexity and time of iterations increases a lot. The convergence has been monitored both with tracking methane concentration at the outlet, following residuals and by visually following plots of important variables. The solutions have been considered converged when the monitored variables were stable and the residuals low enough. This means reasonable converged solutions, where the outcomes should not be significantly influenced.

One aspect that has been overlooked in our simulations is possible transient situations, for example in the start-up process of the reactor. Large fluctuations in the inlet compositions could result in a sudden peak of methane and hydrogen combustion which may increase the flame temperature significantly, up to the region of maximum operational temperature of the refractory bricks (1800 K). Both methane and hydrogen have adiabatic flame temperature over 2000 K in air. Shifting inlet compositions may also occur if there are operation problems encountered in the upstream primary reformer.

In case coking problems are present in the reactor mentioned composition fluctuations also may cause combustion of deposited carbon which will give high temperatures on the catalyst surface. The damages that were observed might be connected to this.

Transient conditions were not investigated due to time restrictions and focus being laid upon primarily simulating the secondary reformer in standard operational conditions.

5.2 Flow distribution and mixing

Obtained simulation results in 3D verify the occurrence of mixing problems in the reactor. Relatively uneven temperature and methane concentration distribution into the catalyst bed could be observed. Not only large radial gradients occurred but also angular variations were noted which arise due to the spacing between the air inlet holes in the burner. Another important observation was the violent impingement of gases towards the catalyst bed surface.

In the 2D simulations sensitivity tests were carried out with respect to the turbulent inlet boundary conditions. Results indicated that despite highly overestimated turbulence inlet properties the flow pattern would remain practically the same with large temperature and concentration gradients at the catalyst surface. The reasons for this is thought to be that the turbulent eddies entering the reactor through the inlets have small length scales in comparison with the reactor dimensions and will not influence flow distribution or mixing significantly. The mixing limiting factors must originate from sources of larger, macroscopic nature.

The 3D simulations where the mass flow rates of each air inlet row are manipulated resulted in significant changes in flow distribution while methane conversion remained constant. Particularly remarkable are the simulations where the air outer inlet row mass flow is increased, resulting in more even temperature and methane concentration profiles across the catalyst inlet. When increasing the air inlet flow through the angled nozzles it appears to disrupt the process gas stream path and enhance mixing. However, as can be observed in Figure 25 the recycling flow near the burner forms a high-temperature region which may cause damage to the burner itself. Thus, these mass flow manipulation tests shouldn’t be regarded as ways of resolving the reactor problem but merely an indicator of the possibility of improving the mixing by optimizing the burner design.

The Danish corporation Haldor Topsøe is a leading producer of catalyst and process technologies for chemical plants and has over years done extensive research on efficient burner designs for auto-thermal secondary reforming (Topsøe, 2010). Figure 28 compares a CFD model of a recently developed ring-type burner designed by Topsøe (left) and the burner used by PT Pusri (right) in their secondary reformer (Pusri-II).

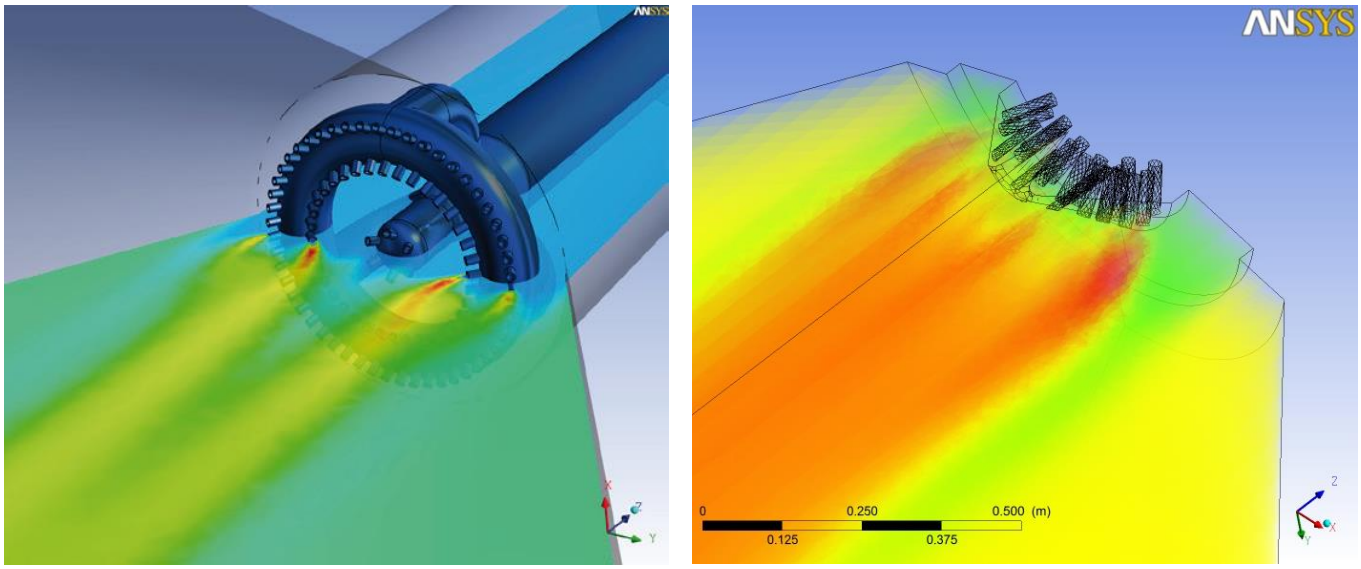

Figure 28.Comparison between CFD models of a Topsøe-designed ring-type burner (left) and the burner used by PT Pusri (right).

The differences are quite evident. The burner developed by Topsøe features inlet nozzles that are all angled with respect to the main process gas stream. Just as the above discussion bring up, such nozzle positions would most likely enhance mixing. Another fundamental difference is the ring-type approach which enables the gas to flow into the center of the combustion zone. This design concept will also result in a more evenly distributed radial temperature profile. Angular variations have also been looked into and were minimized by increasing the number of nozzle inlets in the improved burner.

By contemplating the fact that PT Pusri uses quite old technology dating from 1972 there is no wonder there are large differences compared to new technology. The far-reaching progress in present burner design confirms the possibilities of improving the inadequate mixing of the secondary reformer in Pusri-II.

The importance of an efficient burner is well formulated in a fact sheet from Haldor Topsø (Topsøe, 2010):

"*The efficiency of gas mixing is primarily a function of the burner design. In addition to causing inefficient gas mixing, a poorly designed burner can damage the vessel walls, refractory or even the burner itself due to impingement of hot gas and/or flame in these areas.*"

In the above quote the two main reactor problems that are investigated in this master thesis are brought up as consequences of inadequate burner design. There is no doubt that high outlet concentration of methane originates from this. But it may well be possible that the current burner also is the source to the breakage of refractory bricks and the zone of damaged catalyst under it due to the observed impinging flow of hot gases. Such flow behavior exposes the refractory bricks layer to large strain rates and if they break the catalyst is in turn exposed to the hot flame of temperatures close to the upper limit of the catalyst operational ranges (Appendix: Catalysis specification).

5.3 Material aspects

If we are to regard other alternative factors that may cause methane slip or catalyst failure the possibility of catalyst deactivation processes such as coking and catalyst sintering must be discussed.

Coking is commonly encountered in industry and is favored at elevated temperatures. The phenomenon leads to blockage of active catalyst surface sites, which will hinder the reaction in these points and thus result in inferior methane conversion. Since the reforming reactions are endothermic the solid catalyst will reach higher temperatures when there is little reaction and may result in further catalyst damages. However, the issue with damaged refractory bricks cannot be connected to coking or any other catalyst deactivation process. Occurrence of coking could easily be indicated by increased pressure drop over the catalyst bed or simply through inspection or analysis of damaged catalyst.

Similar arguments can be presented when it comes to catalyst sintering, the active surface area will decrease and decrease methane converted. The catalyst damages that are established in the secondary reformer of Pusri-II are most likely related to sintering due to the exposure to the high temperature flame as the refractory layer is damaged.

Sulphur poisoning should not be an issue since sulphur is removed from the natural gas stream before the reforming process. Therefore has this been neglected in this thesis, but of course can be of importance if there is issues with the purifications step.

As discussed in the precious subchapter it is probable that the impinging flow is one of the main sources to physical damages causing the reactor problems occurring. There is also a possibility of small particles entering the reactor through the inlets could give further negative effects through augmented strain rates imposed on the refractory layer.

One final aspect that cannot be overlooked is simply inadequate material quality of the refractory brick and or the catalyst particles. Both products have to withstand high temperature and intra-material tensions and any quality issues could lead to the reactor problems in the present reactor. Simple tests can be carried out in order to prove or reject material quality being a significant problem. This was previously suggested by Alfa in his report and PT Pusri ought to have performed such analysis.

6 Conclusion

Both 2D and 3D simulations of the combustion zone of the secondary reformer were successfully carried out with reasonable reliability that gives a useful description of the reactor performance and behavior. Simulations of the catalyst zone and the reforming reactors were only made in 2D.

In terms of the problems regarding high methane slip and catalyst failure it can be understood that bad mixing is the major in process caused by inadequate burner design. By comparison of the old burner used from 1972 with a more modern one, it is evident where the significant factor to inadequate mixing lies and the room for improvement of the current burner.

The damage of the catalyst and its protective bricks can most likely be related to the impinging flow, large temperature gradients or bad material quality. To speculate exactly what causes it is not really possible. Material analyses that reject the idea of poor material quality would make it easier to indicate the definite source to the damages. The simulations do not support the idea of local hot spots causing the refractory bricks to break since according to the material specifications, they should withstand temperature far are above the temperature ranges that were obtained in the simulations.

Transient simulations were not carried out; it may well be possible that fluctuations in fuel supply during the start-up process will cause uneven combustion and consequently give peak temperatures that are high enough to damage the refractory bricks and the catalyst. Also composition fluctuations from the primary reformer may cause inferior methane conversion.

7 Further investigation

There is room for continuation and further studies in this work, some ideas are suggested in the list below:

- Test the quality of the bricks and the catalyst
- Investigate occurrence of coking
- Install thermocouple in the middle of the catalyst surface
- Optimize the burner design or evaluate a change to a more modern one
- Include radiation and heat losses in the simulation model
- Improve the UDF by including more accurate mass transport models, to improve reliability of the simulations of the reforming reactions.
- Simulate active catalytic bed in 3D
- Create a CFD model that can simulate both the combustion zone and the active catalyst bed in the same run
- Transient simulations

Some of these bullets were mentioned already in Alfas report. These are still of interest and some of these could be investigated during the next turnover. Other aspects can possibly be investigated in a new master thesis through continued collaboration between the two universities and PT Pusri.

8 Culture of Indonesia

During our four month stay in Yogyakarta, Indonesia, we have had the valuable opportunity of experience the society and the culture at first hand. To be able to work and understand different cultures is an important goal in the engineering education at Chalmers University of Technology.

8.1 Indonesia

The Republic of Indonesia comprises thousands of islands of the large Malay Archipelago located in Southeast Asia. A total population reaching nearly 240 million people makes it the 4th most populous country in the world. But the most remarkable is not the size, but the ethnic and linguistic diversity of the population. Over 700 different languages are spoken by 300 ethnic groups.

The history of Indonesia has been greatly influenced by foreign cultural, political and religious powers since the 7th century when the kingdom of *Sriwijaya* flourished and Hinduism and Buddhism was brought to the region. Centuries later arab traders introduced Islam which eventually became the dominating religion of the nation. European colonial powers were present in the archipelago for over 300 years, attracted by the natural resources. During the World War II Indonesia was occupied by Japanese forces which triggered the national rebellion for independence which was finally declared in 1945.

It's important to understand that despise of the large regional cultural and religious differences, most Indonesians have developed a strong and shared national identity demonstrated by their common language, *Bahasa Indonesia*. This language was created ease communication across the many different native tongues.

Now days the Indonesian economy is progressing rapidly. It is a large economy placed 15th world wide according to the International Monetary Fund, but only placed 104th if ranked per capita. Socioeconomic inequalities are prevalent, both regionally and among the social classes. Its economy is diversified but relies heavily on its natural resources and agriculture. The government takes and active role as owner of several industries in a large range of sectors. It also restricts the activities from foreign corporations and subsidies important commodities such as gasoline and fertilizers.

8.2 Hofstede cultural dimensions

Through the years many researchers have looked into what makes different countries and cultures unique. Many questions remain unanswered and no universal ideas are applicable on the whole world at once. This is connected to that the concept of culture is dynamic and subjective which makes the scientific study very complex.

One of the most commonly used models is the Hofstede cultural dimensions (Hofstede). It divides the national culture into five cultural aspects (originally four, but two extra has been added later on, while only five is considered here). These are describing some of the important characteristics of a country's culture by grading them and they will be used as guidance to which we will connect our own findings. Hofstede has also created a special series of dimensions for organizations, but these are not of relevance here.

Ranking of these factors and comments about Indonesia (and Sweden) are all to be found on the Hofstede Centre's website (Hofstede). Focus is on laid upon the Indonesian culture,

whereas the Swedish comparison will be kept short and only to be seen as a reference mark. All subchapters start with one paragraph that describes the dimension. Subsequent paragraph contain comments from the website and the final paragraphs discusses our own opinion and experiences.

8.2.1 Power Distance Index (PDI)

PDI dimension describes how people in a culture accept inequality among people, mainly regarding power. In a country with high PDI value people will accept highly hierarchic systems where everybody knows its own position. In countries with low PDI value people strive to distribute the power and give everyone the same opportunities.

In this ranking is Indonesia considered to have a high PDI which indicates a hierarchic society. They will use indirect communication, suppress negative feedback and expect their manager give direction in most situations. Sweden is in comparison considered to have a low PDI.

Experiences we have had confirm these statements. Managers have much central power while employees are very liable to given directives. Communication was very indirect and ineffective, something we experienced from our visit at the chemical plant. All high ranked managers live within the plant area in a gated community, while factory employees are forced to live in the city far away from plant. The inequality is apparent but yet seems to be widely accepted and unquestioned.

During our study visit we also had several meetings with different managers which seemed to be unnecessary and involved a lot of indirect communication. However, Farid Elashmawi points out that meetings with top managers are crucial for businesses in countries like Indonesia, the higher ranked persons you been introduced to the easier the progress will be (Elashmawi, 2001). While these meeting seem unnecessary and a waste of time they may indeed be advantageous to impress the right persons and push your own agenda.

8.2.2 Individualism (IDV)

IDV tells if persons in a culture defines themselves as ”I” or ”we”. In highly individualistic countries people expect to take care of them self, while collectivistic societies form groups that exchanges loyalties by taking care of each other.

Indonesia is considered to be of a collectivistic society. Most important is the family, which not only includes the core family but also the elder ones, where parent and child are committed to each other. In contrast, Sweden is a highly individualistic country.

Above statements are easy to observe in Indonesia. The central importance of family can be related to the Muslim dominated society, where e.g. rules for forming new families are quite conservative. Also there is a widespread tendency to not “show off” and not break social norms. This connection is not only seen in family aspects, but also in groups such as the ones formed at universities and work places.

A good illustration of this was observed at the university where a relative of one of the employees fell sick. His colleagues in the university responded by organizing a fundraise to pay for necessary health care. This is partly connected to the lack of good systems for pensions/health insurances/other protective system which we do have in Sweden.

8.2.3 Masculinity/Femininity (MAS)

A society with high masculinity tends to focus on competition, heroism, materialism and other aspects that traditional been seen as masculine. Feministic societies however focus on other type of life qualities and tend to form a more equal society based on consensus.

The index value of MAS for Indonesia placed it in the middle as a country of low masculinity, but not low enough to be considered feminine. Status and success is important, but not necessarily connected to material gain and visible symbols. The position that the person holds is often more important, and a respectable is looked upon. Sweden on the other hand is an extremely feminine country, where consensus and work/life balance are considered important.

Indonesians tend to be quite moderate and not too materialistic focused. Instead they seem to respect people in high positions. In working environment they always put effort into doing well, but at the same time there is this idea that they should not be too effective since there are many others that need occupations. This indicates a masculine way of working, but a feminine way of thinking.

An example of this is our supervisor, Rahman. He is teaching at the Gadjah Mada University and his position makes him well respected in the society. But although he is a lecturer and has a PhD degree he earns about one tenth of his brother who is working in industry, however Rahman is nevertheless regarded of higher social status. He comments this with that he chose a fun work that is highly valued in the society, despite the lower salary.

8.2.4 Uncertainty avoidance (UAI)

The UAI indicates how a culture can handle the fact that the future is unknown and how people with act in relation to that. A culture with high UAI will try to maintain codes and behaviors to minimize uncertainty and will react negatively to ideas that break against normality. On the other side a country of low UAI will have a more relaxed and dynamic approach on uncertainty.

Indonesian people try to never show they are upset and will attempt to avoid any type of direct conflicts. Sometimes a third part is involved to solve conflicts and maintain harmony in work places. They score a medium UAI value while Sweden is lower lower on the scale but not far away.

The conclusion from Hofstedte that they try to avoid conflicts and always appear calmly seems to be true. But they are also nice and helpful to everyone. Compared to Sweden they tend to not strictly follow rules (e.g. in traffic) and keep appointments. Extensive planning and being punctual is not their primary priority. In comparison with Sweden these things are far more important.

An example of avoiding uncertainty is the way people’s choices and opinions are restricted. This is evident in their constitution where they must choose one of the five dominant religions and religion in general is something people tend to keep to themselves.

8.2.5 Long-Term Orientation (LTO)

A country with a high LTO will focus on long term commitments and goals. It will try to save for future needs and long term goals and traditions are regarded important to adapt to new situations. In short-term orientated countries people will live for the day, without putting much thought into the future.

Here Sweden scores 20 and to be considered as short term oriented. Indonesia scores 25 but no additional information is available.

That Indonesia seems to be nearly as short-term oriented as Sweden is not that surprising. People seem to live by the day and long term plans for their lives seem uncommon. On the other hand are for example relationships often committed for life even if after a divorce.

One example of this is a loan the government had for cars some years ago. By just cover of 3% of the total cost people could lend the rest of the money to buy a car with very low rate of interest. Traffic expanded quickly out of control and the government quickly realized their mistake and phased out the loans. The short-term view in this was the idea that everyone should have their own car. In long-term aspect they should have investigated what would happen in the longer run which should have been quite foreseeable. This should also be seen in the light that the government still has not introduced proper public transport in the cities. Instead 20% of the Indonesian budget is spent on subsidizing gasoline for the transport sector, which leads to even more traffic. On the other hand this is a proven way of increasing a country's BNP in short-terms.

8.3 Some Indonesian features

Of course not everything can be included in a simple model with just five dimensions. There are a lot of other things that are important and of interest to describe Indonesian culture. Some of the other aspects that we have faced will be discussed here.

It is important to remember that Indonesian culture is very different from Swedish culture. As mentioned previously the dominating religion is Islam, with a minority of other religions. Since all citizens must choose one of the main religions (atheism is formally not permitted) the country heavily influenced by religious activities. Prayer calls can be heard five times a day and a lot of people follow Islamic rules of life.

Indonesia has only had independency for half a century and the first democratic elections were held just 10 years ago so the democratic society is still something new. Corruption is still a problem but a lot of effort is being put into fighting corruption and lately several high ranked police commanders and politicians are facing the justice system. But there is still a way to go.

The country is developing extremely fast at the moment and according to a McKinsey report (Company, 2012) its consuming class will grow from 45 million people today to 113 million in 2030. This fast development can be seen in both people minds and the country's increasing confidence. But even in 2030 more than half of the country's people will be outside the consumer class, which indicates the huge economic inequalities present. Most likely the large socioeconomic injustice will decrease over time as if the country keeps moving in the right direction.

Another observation in the development is that the country adopts western (popular) culture quickly. Smart phones, music, movies, TV shows etc. is spreading across the country and can be found in most places.

Indonesians are very time optimistic and arranging appointments, professional or personal, can be challenging. The deterministic view on time found in Sweden, is not always to be found here. People may be late and often don't see any problem with it at all. It also happened

that they didn’t show up at all due to prioritizing a meeting with a more important person instead.

Equality between women and men is quite good in Indonesia in our experience. However, it is ranked low in many studies, mainly related to the application of Sharia laws in the province of Aceh and in general conservative views. But women are allowed to work, get education and go into politics. But most positions of significant power are dominated by men in the country and it may take many years for that to change.

Also the traffic is very different from Sweden and is characterized by a very dynamic way of driving and a lot of motorbikes. Walking, cycling and public transport are rare practices. Traffic situations in larger cities are getting out of control with hour-long traffic jams during rush hours.

8.4 Creating a sustainable relationship in Indonesia

To form a sustainable relationship with people or organizations of Indonesian culture of academic, professional or friendly nature there are a number of aspects that we would like to emphasize. The central point is to show understanding to foreign culture and how to adapt to it.

The absolute most important aspect to form a good relationship in Indonesia is to learn the language. The ability to communicate in their language opens people’s minds and gives the opportunity to participate in the society. Even if a lot of Indonesian speaks English, some people prefer their native language. The skill level of English varies a lot in the country, in some places it is practically impossible to communicate in English.

It is important to understand that Indonesia is a diversified country consisting of 240 million spread over a large area and with different cultural background. All people should not be treated in the same way, in the same way that the people in Europe are not the same.

Indonesia has enormous potential for the future and many corporations have already started to show interest in it as one of the countries taking over from China’s total dominance of cheap labor today. Both cheap labor and well educated people can be found here, which opens up for large opportunities. Laws, political stability and freedom of speech still have room for improvement. Foreigners that want to do business the country should mind that they are not automatically well welcomed – this must be seen in the light of many years of western colonialists exploiting the country without giving back to the Indonesian population. But such things change over time.

To get understanding and respect from the people is it extremely important to meet them at their level and try to understand their culture. Indonesians have respect for other cultures and ideas, and in return deserve the same treatment.

References

Andersson, B., Andersson, R., Håkansson, L., Mortensen, M., Sudiyo, R., & van Wachem, B. (2012). *Computational Fluid Dynamics for Engineers*: Cambridge: Cambridge University Press.

ANSYS Inc. (2012). ANSYS FLUENT Theory Guide

Aparicio, L. M. (1997). Transient isotopic studies and microkinetic modeling of methane reforming over nickel catalysts. [Article]. *Journal of Catalysis, 165*(2), 262-274. doi: 10.1006/jcat.1997.1468

Avetisov, A. K., Rostrup-Nielsen, J. R., Kuchaev, V. L., Hansen, J. H. B., Zyskin, A. G., & Shapatina, E. N. (2010). Steady-state kinetics and mechanism of methane reforming with steam and carbon dioxide over Ni catalyst. *Journal of Molecular Catalysis a-Chemical, 315*(2), 155-162. doi: 10.1016/j.molcata.2009.06.013

Cairo University. (2006). 9. Forced Convection Correlations. Retrieved from http://www.pathways.cu.edu.eg/ec/Text-PDF/Part%20B-9.pdf

Chan, S. H., Hoang, D. L., & Ding, O. L. (2005). Transient performance of an autothermal reformer—A 2-D modeling approach. *International Journal of Heat and Mass Transfer*(48), 4205–4214.

Company, M. (2012). The archipelago economy: Unleashing Indonesia's potential.

De Deken J, C., Devos E, F., & Froment G, F. (1982). Steam Reforming of Natural Gas: Intrinsic Kinetics, Diffusional Influences, and Reactor Design *Chemical Reaction Engineering?Boston* (Vol. 196, pp. 181-197): AMERICAN CHEMICAL SOCIETY.

De Wilde, J., & Froment, G. F. (2012). Computational Fluid Dynamics in chemical reactor analysis and design: Application to the ZoneFlow (TM) reactor for methane steam reforming. *Fuel, 100*, 48-56. doi: 10.1016/j.fuel.2011.08.068

Dias, J. A. C., & Assaf, J. M. (2008). Autothermal reforming of methane over Ni/g-Al2O3 promoted with Pd The effect of the Pd source in activity, temperature profile of reactor and in ignition. *Applied Catalysis A: General*(334), 243–250.

Dybkjaer, I. (1995). Tubular reforming and autothermal reforming of natural gas — an overview of available processes. *Fuel Processing Technology, 42*(2-3), 85-107. doi: http://dx.doi.org/10.1016/0378-3820(94)00099-F

Elashmawi, F. (2001). *Competing Globally: Mastering Multicultural Management and Negotiations*: Taylor and Francis.

Fazeli, A., & Behnamy, M. (2007). CFD Modeling of Methane Autothermal Reforming in a Catalytic Microreactor. *INTERNATIONAL JOURNAL OF CHEMICAL REACTOR ENGINEERING, 5*.

Hofstede, G. THE HOFSTEDE CENTRE Retrieved 01 May, 2013, from http://geert-hofstede.com/

Lee., J. (2006, July 9, 2008). Nitrogen Fertilizer, Forms and Methods of Application Retrieved April 16, 2013, from http://www1.agric.gov.ab.ca/$department/deptdocs.nsf/all/ind10750

Rasmusson A, e. a. (2010). *Course book: Matematisk modellering*: Chemical engineering, Chalmers.

Rostrup-Nielsen, J. (1975). Mechanisms of Carbon Formation on Nickel-Containing Catalysts. *Journal of Catalysis, 48*, 155-165.

Schnitzlein, K. (2001). Modelling radial dispersion in terms of the local structure of packed beds. *Chemical Engineering Science, 56*, 579-585.

Sehested, J., Gelten, J. A. P., Remediakis, I. N., Bengaard, H., & Nørskov, J. K. (2004). Sintering of nickel steam-reforming catalysts: effects of temperature and steam and hydrogen pressures. *Journal of Catalysis 223*, 432–443.

Swaminathan, B., & Sukalac, K. E. (2004). *Technology transfer and mitigation of climate change: The fertilizer industry perspective.* Paper presented at the IPCC Expert Meeting on Industrial Technology Development, Transfer and Diffusion, Tokyo, Japan.

Topsoe. (2013). Research Retrieved April, 2013, from http://www.topsoe.com/business_areas/ammonia/research.aspx

Topsøe, H. (2010). Topsøe ammonia technology (PDF). Retrieved from http://www.topsoe.com/business_areas/ammonia/~/media/PDF%20files/Ammonia/topsoe_ammonia_technology.ashx

Trimm, D. L. (1997). Coke formation and minimisation during steam reforming reactions. *Catalysis Today, 37*, 233-238.

Warnatz, J. (1981). *The structure of laminar alkane-, alkene-, and acetylene flames.* Paper presented at the Eighteenth Symposium (International) on Combustion.

Xu, J., & Froment, G. F. (1989). Methane Steam Reforming, Methanation and Water-Gas Shift: 1. Intrinsic Kinetics. *AIChE Journal, 35*(1), 88-96.

Yu, Y. H. (2002). Simulation of secondary reformer in industrial ammonia plant. [Article]. *Chemical Engineering & Technology, 25*(3), 307-314. doi: 10.1002/1521-4125(200203)25:3<307::aid-ceat307>3.0.co;2-c

Nomenclature

C	Constant
C_1	Coefficient for inertial resistance (used in fluent) $[-]$
C_2	Coefficient for viscous resistance (used in fluent) $[-]$
C_ε	Closure coefficient
c_i	Concentration of species i $\left[\frac{mole}{m^3}\right]$
D_p, d_p	Equivalent spherical diameter of the catalysts $[m]$
D, D_{radial}	Diffusivity $\left[\frac{m^2}{s}\right]$
G	Gravity $\left[\frac{m}{s^2}\right]$
h	Convective heat transfer coefficient $\left[\frac{W}{m^2 K}\right]$
I	Turbulent intensity
K_i	Equilibrium coefficient of species i
k	Turbulent kinetic energy $\left[\frac{m^2}{s^2}\right]$
k	Thermal conductivity $\left[\frac{W}{m \cdot K}\right]$
k_i	Kinetic coefficient
L	Length of catalytic bed $[m]$
p_i	Partial pressure of species i $[Pa]$
R	Diameter $[m]$
r_i	Reaction rate
S	Source term
u	Velocity $\left[\frac{m}{s}\right]$
v_z	Axial velocity $\left[\frac{m}{s}\right]$
v_∞	Superficial velocity $\left[\frac{m}{s}\right]$

Greek symbols

γ	Bed porosity $[-]$
Δp	Pressure drop over catalytic bed $[Pa]$
δ	Delta function
ε	Dissipation rate $[m^2/s^3]$
ϵ	Void fraction of the bed $[-]$
μ	Viscosity $[Pa \cdot s]$
v_T	Turbulent viscosity $[Pa \cdot s]$
ρ	Density $\left[\frac{kg}{m^3}\right]$
τ_{axial}	Time constant axial flux $[s]$
τ_{radial}	Time constant radial diffusion $[s]$
φ	PDF

Dimensionless numbers

Da	Damköhlers number
Nu	Nusselt number
Re	Reynolds number

Appendix: Setup simulations

The final setup follows:

Table 10 Final setup of the simulations. The final simulations divides the simulations into two steps where first the whole reformer is simulated. In this is no reactions in the catalyst included and therefore are one profile copied from the interface burner – catalyst. This profile is then used in a second simulation that only simulates the catalyst and its reactions. For the two setups are slightly different models used.

	Burner + inert catalyst	**Active catalyst**
Viscous model	k-epsilon realizable	
Wall function	Non-equilibrium	
Species model	partially premixed combustion, non-adiabatic	Species transport
Catalyst	Porous bed	Porous bed
Catalyst – thermal model	Equilibrium thermal model	Non-equilibrium thermal model (requires separated fluid and solid zones)
Source terms	None	Reaction, energy, heat transfer coefficient (defined by UDF)
Inlet	Mass flow inlet	Pressure inlet (defined by profile copied from hole system)
Outlet	Pressure outlet	Pressure outlet
Pressure-Velocity scheme	SIMPLE	SIMPLE
Numerical scheme	Second order upwind	Second order upwind

Table 11. Process data for the inlet to the reactor. These settings have also been used in the simulations.

	Unit	**Gas inlet**	**Air inlet**
CH4	mol-%	8.66	
CO	mol-%	0.97	
CO2	mol-%	9.30	
H2	mol-%	40.09	
H2O	mol-%	40.99	33.06
O2	mol-%		14.06
N2	mol-%		52.88
Temperature	°C	785	480
Flow rate	kg/h	74560	42228
Pressure	Kg/cm^2,g	28.5	28.95

Appendix: Catalysis specification

The catalyst is built from perforated spheres and is illustrated in Figure 2. The figure is just an illustration and in reality are the ends slightly convex. More details can be found in Table 12.

Table 12. Catalysis specification

Dimensions spheres [mm]	16.5 x 18.0
Dimensions holes [mm]	7 x 3.4
Number of holes	7
Shape	Spheres with convex ends
Composition	89% Alumina (Al2O3) 10.5% NiO Small fractions of Al2O4, Al2O5, Al2O6, SiO2 are also present
Bulk density [kg/lt]	0.9 ± 1
Operating temperature [°C]	400 - 1300
Operating pressure [Bar]	40

Appendix: UDF

```
#include <udf.h>

//                      Constants
real R=8.314;                           // [J/K,mol]
real M_CH4=0.0160425;                   // [kg/mol]
real M_H2=0.00201588;                   // [kg/mol]
real M_H2O=0.0180153;                   // [kg/mol]
real M_CO=0.0280101;                    // [kg/mol]
real M_CO2=0.0440095;                   // [kg/mol]

//                      Operating pressure
real P_op=2896000.;                     // [Pa]

//                      Variables
real T,P,rho,C_tot,y_CH4,y_CO,y_CO2,y_H2,y_H2O,P_CH4,P_CO,P_CO2,P_H2,P_H2O,r_1,r_2,r_3,flag,dH1,dH2,dH3,heat_gen,kf; //
Temperature, pressure, total concentration
real A_k[3],A_K[4],E[3],delta_H[3],k[3],K[4],Ke[3],eff_fact,T_b;

enum{co,co2,ch4,h2,h2o};

DEFINE_SOURCE(CO_rxrate,c,t,dS,eqn)
{
                        Domain *sol_domain;                             // Defines the correct domain and threads
                        Thread *sol_thread;
                        Domain *flu_domain;
                        Thread *flu_thread;

                        real DEN,P_tot;
                        int i;

                        sol_domain = Get_Domain(1);
                        sol_thread = Lookup_Thread(sol_domain,7);
                        flu_domain = Get_Domain(1);
                        flu_thread = Lookup_Thread(flu_domain,4);

                        eff_fact = 3.4e-6;                              // Global efficiency factor

                        T=C_T(c,sol_thread);                            // Temperature
                        T_b = C_T(c,t);

                        rho=C_R(c,t);                                   // Density
                        P_tot=C_P(c,t)+P_op;                            // Pressure
                        C_tot=P_tot/R/T_b;// [mol/m3]                   // Concentration
                        k[0] = 1.17e15*exp(-240100/R/T);                // Kinetic coefficient
                        k[1] = 5.43e5*exp(-67130/R/T);
                        k[2] = 2.83e14*exp(-243900/R/T);

                        K[0] = 8.23e-5*exp(8497.71/T);                  // Equilibrium constant
                        K[1] = 6.12e-9*exp(9971.13/T);
                        K[2] = 1.77e5*exp(-10666.35/T);
                        K[0] = 6.65e-4*exp(4604.28/T);

                        Ke[0] = exp((-26830/T)+30.114);                 // Jämviktkonst. Approximation from earlier work at UGM
                        Ke[1] = exp((4400/T)-4.063);                    // Equilibrium constant
                        Ke[2] = Ke[0]*Ke[1];

                        y_CH4=C_YI(c,t,ch4)*rho/M_CH4/C_tot;            // molar fraction CH4
                        y_CO=C_YI(c,t,co)*rho/M_CO/C_tot;               // CO
                        y_CO2=C_YI(c,t,co2)*rho/M_CO2/C_tot;            // CO2
                        y_H2=C_YI(c,t,h2)*rho/M_H2/C_tot;               // H2
                        y_H2O=C_YI(c,t,h2o)*rho/M_H2O/C_tot;            // H2O

                        P_CO=P_tot*y_CO/1e5;                            // Partial pressure [Bar]
                        P_CO2=P_tot*y_CO2/1e5;
                        P_CH4=P_tot*y_CH4/1e5;
                        P_H2O=P_tot*y_H2O/1e5;
                        P_H2=P_tot*y_H2/1e5;
```

```
		flag = 0;				// In case no hydrogen -> no reaction (assumption)
		if(y_H2 <= 1e-3)
		{		P_H2 = P_tot/1e5/100;
				flag = 1;		}

				DEN=1+K[0]*P_CO+K[1]*P_H2+K[3]*P_CH4+K[2]*P_H2O/P_H2;		// Needed for
calculations

				r_1=eff_fact*((k[0]/pow(P_H2,2.5))*(P_CH4*P_H2O-pow(P_H2,3.)*P_CO/Ke[0]))/pow(DEN,2.);

				r_2=eff_fact*((k[1]/P_H2)*(P_CO*P_H2O-P_H2*P_CO2/Ke[1]))/pow(DEN,2.);
				r_3=eff_fact*((k[2]/pow(P_H2,3.5))*(P_CH4*pow(P_H2O,2.)-
pow(P_H2,4.)*P_CO2/Ke[2]))/pow(DEN,2.);

				if (flag == 1)
{
				r_1=0.;
				r_2=0.;
				r_3=0.;

		}

		dS[eqn]=0.;
		C_UDMI(c,t,0)=r_1;						// Save reaction rates
		C_UDMI(c,t,1)=r_2;
		C_UDMI(c,t,2)=r_3;

		r_1=C_UDMI(c,t,0);
		r_2=C_UDMI(c,t,1);
		r_3=C_UDMI(c,t,2);

		return 1900*1000*(r_1-r_2)*M_CO;			// [kg/m3,s]
}

DEFINE_SOURCE(CO2_rxrate,c,t,dS,eqn)
{
		r_1=C_UDMI(c,t,0);
		r_2=C_UDMI(c,t,1);
		r_3=C_UDMI(c,t,2);
		return 1900*1000*(r_2+r_3)*M_CO2;			// [kg/m3,s]
}

DEFINE_SOURCE(CH4_rxrate,c,t,dS,eqn)
{
		r_1=C_UDMI(c,t,0);
		r_2=C_UDMI(c,t,1);
		r_3=C_UDMI(c,t,2);
		return 1900*1000*(-r_1-r_3)*M_CH4;			// [kg/m3,s]
}

DEFINE_SOURCE(H2_rxrate,c,t,dS,eqn)
{
		return 1900*1000*(3*r_1+r_2+4*r_3)*M_H2;		// [kg/m3,s]
}

DEFINE_SOURCE(H2O_rxrate,c,t,dS,eqn)
{
		r_1=C_UDMI(c,t,0);
		r_2=C_UDMI(c,t,1);
		r_3=C_UDMI(c,t,2);
		return 1900*1000*(-r_1-r_2-2*r_3)*M_H2O;		// [kg/m3,s]
}

DEFINE_SOURCE(solid_energy,c,solid_thread,dS,eqn)
{
		Domain *solid_domain;
		Thread *solid_thread;
		Domain *fluid_domain;
		Thread *fluid_thread;
```

```
		solid_domain = Get_Domain(1);
		solid_thread = Lookup_Thread(solid_domain,7);
		fluid_domain = Get_Domain(1);
		fluid_thread = Lookup_Thread(fluid_domain,4);

		dH1=206.1;				// kJ/mol
		dH2=-41.15;
		dH3=164.9;

		r_1=C_UDMI(c,fluid_thread,0);
		r_2=C_UDMI(c,fluid_thread,1);
		r_3=C_UDMI(c,fluid_thread,2);

		C_UDMI(c,fluid_thread,3)=-1900*1000*(r_1*dH1 + r_2*dH2 + r_3*dH3);

		return 1900*1000*(r_1*dH1 + r_2*dH2 + r_3*dH3);

}

DEFINE_PROFILE(c_coeff,f_thread,i)
{
		Domain *f_domain;
		Thread *f_thread;


		real x[ND_ND];
		real y;
		cell_t c;

		f_domain = Get_Domain(1);
		f_thread = Lookup_Thread(f_domain,4);

		begin_c_loop(c,f_thread)
		{
			C_CENTROID(x,c,f_thread);
			y = x[1];
			C_PROFILE(c,f_thread,i) =
1.09/0.5*pow(C_U(c,f_thread)*0.0225*C_R(c,f_thread)/C_MU_L(c,f_thread),1/3)*pow(C_MU_L(c,f_thread)/(2.88e-
5*pow((C_T(c,f_thread)/(60+273)),1.75)*(1e5/(C_P(c,f_thread)+101325))*C_R(c,f_thread)),1/3)*C_K_L(c,f_thread)/0.0225;
			C_UDMI(c,f_thread,4) = C_PROFILE(c,f_thread,i);
		}
		end_c_loop(c,f_thread)


}
```

Appendix: Air inlet sensitivity analysis; mean mixture fraction across catalyst surface

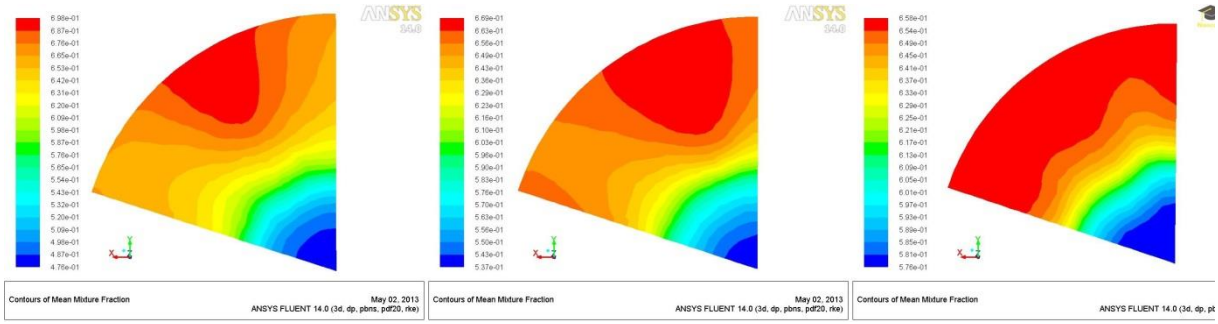

Figure 29. Local contour values of mean mixture fraction across the catalyst inlet surface. Increased air inlet row mass flow, left to right: inner +20%, middle +20%, outer +20%.

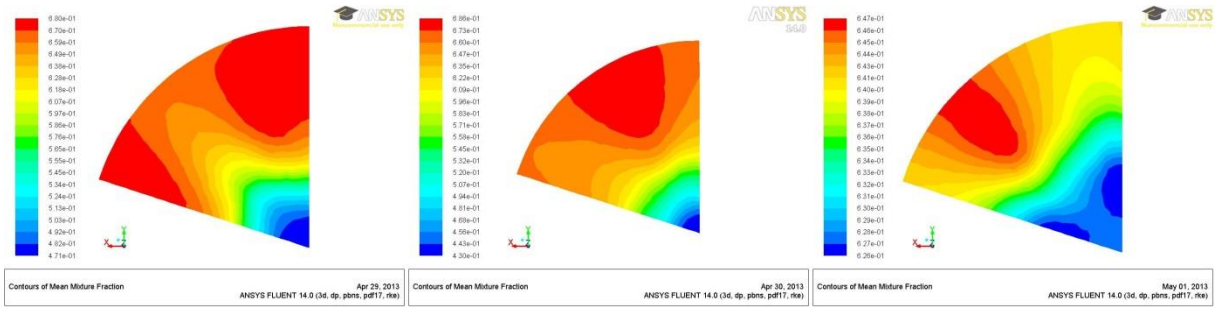

Figure 30. Local contour values of mean mixture fraction across the catalyst inlet surface. Increased air inlet mass flow of rows, left to right: inner/middle +20%, inner/outer +20%, middle/outer +10%.